DMD DRUG METABOLISM AND DISPOSITION aspet

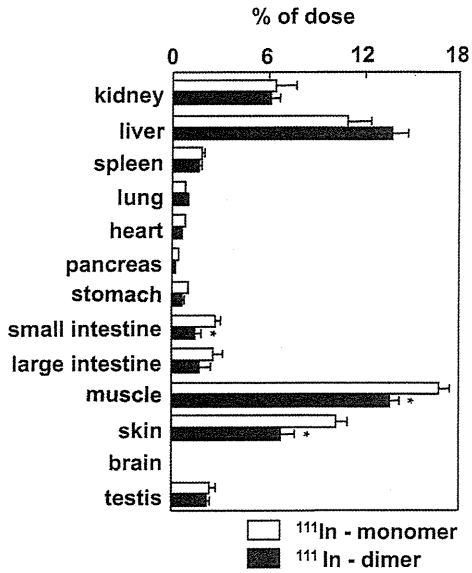

FIG. 3. Tissue distribution of radioactivity at 48 h after the intravenous administration of ^{111}In-HSA monomer or dimer to normal rats. ^{111}In-HSA monomer (open bars) or ^{111}In-HSA dimer (closed bars) was injected at a dose of 1 mg/kg. Each bar represents the mean ± S.D. (n = 6). *, $p < 0.05$ versus ^{111}In-monomer.

The radioactivities of ^{111}In at 48 h after administration of the HSA monomer and dimer were negligible (4.9 ± 0.2 and 3.3 ± 1.7% of ID for the HSA monomer and dimer, respectively; no significant differences).

Pharmacokinetics of HSA Monomer and Dimer in Nephrotic Rats. A pharmacokinetics study of the HSA dimer was also performed in nephrotic rats induced by doxorubicin treatment. The serum albumin level in nephrotic rats was 3.41 ± 0.2 g/dl (versus normal rats; 3.74 ± 0.2 g/dl, no significant differences), and urinary protein was 213 ± 28 mg/day (versus normal rats; 8.0 ± 3.4 mg/day, $p <$ 0.001). These data are consistent with a previous report (Bertani et al., 1982) and indicate that nephrosis was induced in the doxorubicin-treated rats.

As shown in Fig. 4 and Table 2, the plasma concentration of HSA monomer was rapidly cleared compared to that of the HSA dimer in nephrotic rats (13.5 ± 2.4 and 7.0 ± 1.9 h, $p < 0.01$, for the HSA dimer and monomer, respectively), whereas the plasma concentration of the HSA dimer in nephrotic rats was similar to that in normal rats. The CL for the HSA dimer was decreased to one-third of the HSA monomer (0.56 ± 0.1 and 1.8 ± 0.4 ml/h, $p < 0.05$, for the HSA dimer and monomer, respectively). The AUC was also significantly increased (177 ± 15 and 56 ± 6.0 h · % of dose/ml, $p < 0.01$, for the HSA dimer and monomer, respectively).

TABLE 2

Pharmacokinetic parameters after administration of ^{111}In-rHSA monomer and dimer after intravenous administration to nephrotic model rats

All nephrotic model rats received a single injection of ^{111}In-rHSA monomer or dimer at a dose of 1 mg/kg. At each time after the injection of ^{111}In-rHSA monomer or dimer, a blood sample was collected from the tail vein and plasma was obtained. Each parameter was calculated by MULTI using a two-compartment model. Each value represents the mean ± S.D. (n = 6).

	^{111}In-Monomer	^{111}In-Dimer
$t_{1/2}$ (h)	7.0 ± 1.9	13.5 ± 2.4**
AUC (h · % of dose/ml)	56 ± 15	177 ± 15**
CL (ml/h)	1.8 ± 0.4	0.56 ± 0.1*
V_{dss} (ml)	15.3 ± 0.7	13.5 ± 0.3
Renal CL (ml/h)	1.8 ± 0.5	0.20 ± 0.12**

* $p < 0.05$ and ** $p < 0.01$ versus ^{111}In-monomer.

As shown in Fig. 5, the HSA monomer and dimer were both mainly distributed in the kidney, liver, skin, and muscle, the same as that in normal rats. Among these organs, there were no significant differences between the accumulation of the HSA monomer and dimer in liver, skin, and muscle. Note that the accumulation of the HSA dimer in the kidney was dramatically decreased compared to that of the HSA monomer.

The urinary excretion of ^{111}In in nephrotic rats was also measured (Fig. 6). The radioactivity of ^{111}In after administration of the HSA monomer was 75.1 ± 13.0% of ID at 48 h, whereas the radioactivity after HSA dimer administration was decreased by half compared to that after the administration of the HSA monomer (34.6 ± 20% of ID at 48 h after injection, $p < 0.05$). In addition, the renal CL of HSA monomer was 1.81 ± 0.46 ml/h, whereas that of HSA dimer was 0.20 ± 0.12 ml/h in nephrotic rats.

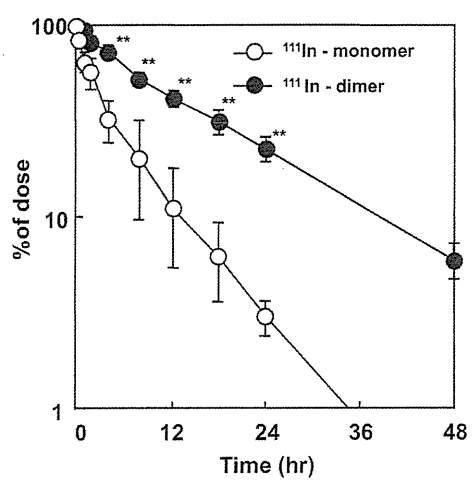

FIG. 4. Relative plasma concentration of ^{111}In-HSA monomer and dimer after intravenous administration to nephrotic rats. ^{111}In-HSA monomer (open circles) or ^{111}In-HSA dimer (closed circles) was injected at a dose of 1 mg/kg. Each point represents the mean ± S.D. (n = 6). **, $p < 0.01$ versus ^{111}In-HSA monomer.

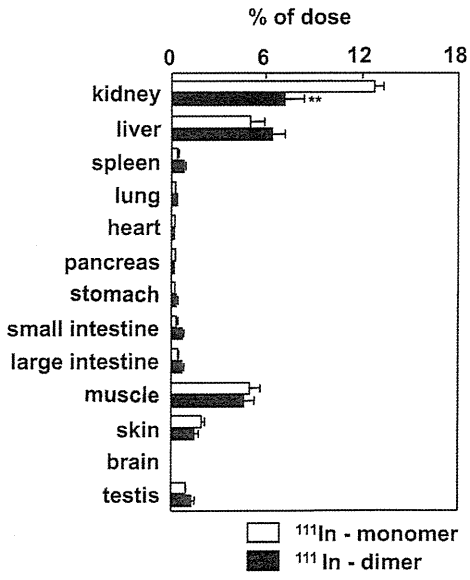

FIG. 5. Tissue distribution of radioactivity at 48 h after intravenous administration of ^{111}In-HSA monomer or dimer to nephrotic rats. ^{111}In-HSA monomer (open bars) or ^{111}In-HSA dimer (closed bars) was injected at a dose of 1 mg/kg. Each bar represents the mean ± S.D. (n = 6). **, $p < 0.01$ versus ^{111}In-monomer.

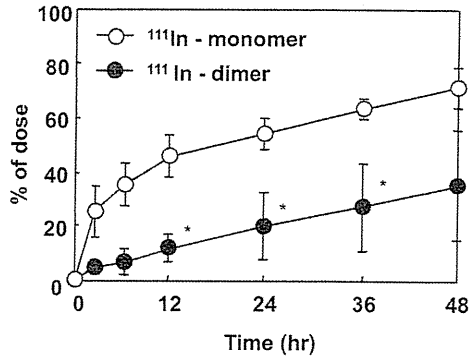

FIG. 6. Urinary excretion of ^{111}In-rHSA monomer and ^{111}In-rHSA dimer after intravenous administration to nephrotic rats. ^{111}In-HSA monomer (open circles) or ^{111}In-HSA dimer (closed circles) was injected at a dose of 1 mg/kg. Each point represents the mean ± S.D. (n = 4). *, $p < 0.05$ versus ^{111}In-monomer.

Discussion

The major finding of this study is that the HSA dimer has the ability to maintain the blood retention properties as well as that reported for normal conditions, even though under the high-permeability conditions, such as nephrosis, it can be expected to function as a novel plasma expander.

In the case of normal rats, the $t_{1/2}$ for the HSA dimer (17.2 ± 2.5 h) was 1.3 times higher than that of the HSA monomer (13.3 ± 1.8 h) accompanied by a decrease in the clearance from circulation. It is generally known that approximately 40% of native albumin exists in the vascular space, and the remaining 60% is present in the extravascular space. This ratio is equilibrated between each space through the vascular endothelium. Our data suggest that the movement of the HSA dimer from the vascular space to the cellular space through the vascular endothelium is suppressed, and the molecular mass of the dimer is double that of the monomer (Fig. 1). In fact, in normal rats, the V_{dss} value for the HSA dimer (13.9 ± 0.3 ml) was significantly decreased compared to that for the HSA monomer (15.5 ± 0.2 ml). As a result, the accumulation of HSA dimer in skin and muscle was significantly suppressed compared with the corresponding values for the HSA monomer (Fig. 3). This conclusion is supported by the findings reported from Matsushita et al. (2006), who fused two molecules of HSA to produce a recombinant HSA dimer using a yeast expression system. They clearly showed that the plasma $t_{1/2}$ of the recombinant HSA dimer was prolonged by 1.1 times due to a decrease in the vascular permeability of the HSA dimer compared to that for the HSA monomer in carrageenin-air-pouch rats. Moreover, Sejrsen et al. (1985) reported that the predominant transcapillary transport mechanism for ^{131}I-albumin is compatible with transcapillary diffusion through pores with an effective equivalent pore radius of 145 Å. Hence, the extent of extravasation of albumin may be reduced by increasing its molecular size. It has also been shown that albumin, with an estimated radius of 35.5 Å, and water do not share a common pathway in crossing the endothelial monolayer, suggesting the existence of a large pore pathway for albumin (Dull et al., 1991). Namely, the increase in the molecular size of HSA clearly led to retardation in extravasation through the vascular endothelium, resulting in a longer lifetime in the blood stream.

In the cases of certain renal injuries or obstacles, such as nephrotic syndrome, infused HSA is easily filtered by the renal glomerulus. In contrast, the $t_{1/2}$ for the HSA dimer in nephrotic rats (13.5 ± 2.4 h) was comparable to that for the HSA monomer (13.3 ± 1.8 h) in normal rats. Thus, the $t_{1/2}$ for the HSA dimer was approximately double that of the HSA monomer in nephrotic rats (7.0 ± 1.9 h). In general, the glomerular biological membrane has properties that allow for high filtration rates of water and small and mid-sized molecules but does not allow larger proteins such as HSA to be filtered. These restrictions can be explained by several mechanisms, including charge repulsion in the glomerular basement membrane and barrier, depending on their molecular sizes (Haraldsson et al., 2008). The molecular mass of the HSA dimer is exactly 132,741 Da, and the HSA dimer retains a negative charge as well as the HSA monomer (pI = 4.8) (Komatsu et al., 2004a). Therefore, the increased $t_{1/2}$ for the HSA dimer in nephrotic rats is likely to be due to the increased molecular size of the molecule. In fact, several results in this study support this hypothesis: 1) the renal distribution and urinary excretion of the HSA dimer were decreased significantly compared to those of the HSA monomer (Figs. 5 and 6); 2) the renal accumulation of the HSA dimer in nephrotic rats was similar to that in normal rats (Figs. 3 and 5); and 3) after administration of the HSA dimer to nephrotic rats, the reduction in urinary excretion prolonged the $t_{1/2}$ (Figs. 4 and 6). Although the renal CL of HSA monomer was consistent with the systemic CL of HSA monomer in nephrotic rats, the renal CL of HSA dimer was lower than the systemic CL of HSA dimer. This result suggested that the increased $t_{1/2}$ of HSA dimer in nephrotic rats was not explained by only suppression of protein leakage across the glomerulus. In the previous reports, bone was one of the major distribution tissues of albumin (Yedgar et al., 1983) and albumin was a constituent of the organic matrix in bone (Triffitt and Owen, 1973). Therefore, HSA dimer may be distributed and used in bone. However, in this study, we could not examine the clearance of HSA in bone. Further study will be needed to achieve this issue.

Martini et al. (2008) demonstrated a new type of plasma expander, PEG-HSA (carrying six copies of PEG-5000 chains per molecule; molecular mass, 97 kDa), that is effective at reduced plasma concentrations and potentially has a better defined pharmacokinetic profile because of its larger molecular size. Furthermore, the researchers suggested that the PEGylation of HSA possibly results in a more effective plasma volume expander during hemodilution or in resuscitation fluids that are used for the treatment of hemorrhagic shock with the advantages of a longer $t_{1/2}$ because of reduced glomerular filtration and movement to the extravascular space. Because the molecular mass of the HSA dimer is approximately 130 kDa, which is larger than the PEG-HSA alluded to above, it has promise as a new plasma volume expander instead of native HSA monomer for patients with hypoalbuminemia, especially nephrotic syndrome.

As described above, because the HSA dimer shows superior blood retention properties, it would be also expected to serve as a carrier for drug delivery in high-permeability conditions. Tsuchida et al. (1997) previously reported on an HSA-based artificial oxygen carrier "albumin-heme (HSA-FeP)," which is a synthetic heme with a covalently bound proximal base that is incorporated into the hydrophobic cavities of HSA. HSA-FeP reversibly binds and releases O_2 under physiological conditions, the same as hemoglobin (Komatsu et al., 1999). An in vivo study using hemorrhagic shocked rats revealed that the renal cortical O_2-tensions and skeletal tissue O_2-tensions were increased when HSA-FeP was injected (Tsuchida et al., 2000; Komatsu et al., 2004b). An artificial oxygen carrier is also required to maintain high blood circulation, because it must temporarily function until a blood transfusion is available or until autologous blood is recovered after a massive hemorrhage. In fact, we demonstrated previously that the HSA dimer enables a maximum of 16 molecules of FeP to bind and the obtained dimeric HSA-FeP bound oxygen approximately twice higher than blood (Komatsu et al., 2004a). The HSA-FeP dimer shows promise as a new type of oxygen carrier that is efficiently retained in circulating blood under nephrotic conditions. Although this study

Downloaded from dmd.aspetjournals.org at Keio University Shinanomachi Media Center on May 12, 2011

DMD
DRUG METABOLISM AND DISPOSITION
aspet

provides a demonstration of the utility of the HSA dimer as a plasma expander, our model has several limitations with respect to extrapolating it for use in a human clinical setting. Our studies only dealt with nephrotic syndrome, as induced by doxorubicin. Because nephrotic syndrome is a multiplex pathology induced by several factors, such as heredity and immunity, it will be necessary to demonstrate the pharmacokinetic properties of the HSA dimer in several nephrotic syndrome model animals. In addition, the dose used in this study (1 mg/kg) is less than a pharmacologic dose in a clinical situation. A pharmacokinetic examination using pharmacologic doses of monomer and dimer should be one of the subjects of future investigation. Moreover, recent evidence indicates that the Fc receptor (FcRn) expressed in the kidney reclaimed albumin, thus maintaining the serum concentration of albumin (Sarav et al., 2009). This finding indicates that interactions between albumin and FcRn are important aspects of the pharmacokinetics of albumin. However, it is well established that there is a large species difference in the interaction of albumin and FcRn. In this study, because human albumin was administrated to rats, the interaction between HSA and rat FcRn would likely be negligible. Thus, this interaction is not likely to contribute to the pharmacokinetic data related to the HSA dimer as shown in this study. However, it will be necessary to examine the interactions of the HSA dimer and human FcRn for clinical development.

In conclusion, the cross-linked HSA dimer shows potential for use as a new plasma volume expander, because it showed superior blood retention characteristics in various clinical situations. Its use would allow us to reduce the multiple administrations required in the case of conventional HSA preparations and could be quite cost-effective. In addition, the HSA dimer is also predicted to function as a versatile carrier for drug delivery systems, in particular, an albumin-based artificial oxygen carrier. Recombinant HSA has very recently been approved as a serum-derived HSA alternative in Japan. As a result, it seems likely that a recombinant HSA dimer could be used as a substitute of HSA preparations, even in cases of various pathological conditions such as nephrotic syndrome.

References

Andersson LO (1970) Hydrolysis of disulfide bonds in weakly alkaline media. II. Bovine serum albumin dimer. *Biochim Biophys Acta* **200:**363–369.

Bertani T, Poggi A, Pozzoni R, Delaini F, Sacchi G, Thoua Y, Mecca G, Remuzzi G, and Donati MB (1982) Adriamycin-induced nephrotic syndrome in rats: sequence of pathologic events. *Lab Invest* **46:**16–23.

Bradford MM (1976) A rapid and sensitive method for the quantitation of microgram quantities of protein utilizing the principle of protein-dye binding. *Anal Biochem* **72:**248–254.

Cochrane Injuries Group Albumin Reviewers (1998) Human albumin administration in critically ill patients: systematic review of randomised controlled trials. *BMJ* **317:**235–240.

Doumas BT, Watson WA, and Biggs HG (1971) Albumin standards and the measurement of serum albumin with bromcresol green. *Clin Chim Acta* **31:**87–96.

Dull RO, Jo H, Sill H, Hollis TM, and Tarbell JM (1991) The effect of varying albumin concentration and hydrostatic pressure on hydraulic conductivity and albumin permeability of cultured endothelial monolayers. *Microvasc Res* **41:**390–407.

Haraldsson B, Nyström J, and Deen WM (2008) Properties of the glomerular barrier and mechanisms of proteinuria. *Physiol Rev* **88:**451–487.

Hnatowich DJ, Layne WW, and Childs RL (1982) The preparation and labeling of DTPA-coupled albumin. *Int J Appl Radiat Isot* **33:**327–332.

Komatsu T, Hamamatsu K, Wu J, and Tsuchida E (1999) Physicochemical properties and O2-coordination structure of human serum albumin incorporating tetrakis(o-pivalamido)phenylporphyrinatoiron(II) derivatives. *Bioconjug Chem* **10:**82–86.

Komatsu T, Oguro Y, Teramura Y, Takeoka S, Okai J, Anraku M, Otagiri M, and Tsuchida E (2004a) Physicochemical characterization of cross-linked human serum albumin dimer and its synthetic heme hybrid as an oxygen carrier. *Biochim Biophys Acta* **1675:**21–31.

Komatsu T, Yamamoto H, Huang Y, Horinouchi H, Kobayashi K, and Tsuchida E (2004b) Exchange transfusion with synthetic oxygen-carrying plasma protein "albumin-heme" into an acute anemia rat model after seventy-percent hemodilution. *J Biomed Mater Res A* **71:**644–651.

Martini J, Cabrales P, K A, Acharya SA, Intaglietta M, and Tsai AG (2008) Survival time in severe hemorrhagic shock after perioperative hemodilution is longer with PEG-conjugated human serum albumin than with HES 130/0.4: a microvascular perspective. *Crit Care* **12:**R54.

Matsushita S, Chuang VT, Kanazawa M, Tanase S, Kawai K, Maruyama T, Suenaga A, and Otagiri M (2006) Recombinant human serum albumin dimer has high blood circulation activity and low vascular permeability in comparison with native human serum albumin. *Pharm Res* **23:**882–891.

Pulimood TB and Park GR (2000) Debate: Albumin administration should be avoided in the critically ill. *Crit Care* **4:**151–155.

Sarav M, Wang Y, Hack BK, Chang A, Jensen M, Bao L, and Quigg RJ (2009) Renal FcRn reclaims albumin but facilitates elimination of IgG. *J Am Soc Nephrol* **20:**1941–1952.

Sejrsen P, Paaske WP, and Henriksen O (1985) Capillary permeability of 131I-albumin in skeletal muscle. *Microvasc Res* **29:**265–281.

Sollenne NP, Wu HL, and Means GE (1981) Disruption of the tryptophan binding site in the human serum albumin dimer. *Arch Biochem Biophys* **207:**264–269.

Taguchi K, Maruyama T, Iwao Y, Sakai H, Kobayashi K, Horinouchi H, Tsuchida E, Kai T, and Otagiri M (2009) Pharmacokinetics of single and repeated injection of hemoglobin-vesicles in hemorrhagic shock rat model. *J Control Release* **136:**232–239.

Triffitt JT and Owen M (1973) Studies on bone matrix glycoproteins. Incorporation of (1–14C)glucosamine and plasma (14C)glycoprotein into rabbit cortical bone. *Biochem J* **136:**125–134.

Tsuchida E, Ando K, Maejima H, Kawai N, Komatsu T, Takeoka S, and Nishide H (1997) Properties of and oxygen binding by albumin-tetraphenylporphyrinatoiron(II) derivative complexes. *Bioconjug Chem* **8:**534–538.

Tsuchida E, Komatsu T, Hamamatsu K, Matsukawa Y, Tajima A, Yoshizu A, Izumi Y, and Kobayashi K (2000) Exchange transfusion with albumin-heme as an artificial O2-infusion into anesthetized rats: physiological responses, O2-delivery, and reduction of the oxidized hemin sites by red blood cells. *Bioconjug Chem* **11:**46–50.

Vincent JL, Navickis RJ, and Wilkes MM (2004) Morbidity in hospitalized patients receiving human albumin: a meta-analysis of randomized, controlled trials. *Crit Care Med* **32:**2029–2038.

Wilkes MM and Navickis RJ (2001) Patient survival after human albumin administration. A meta-analysis of randomized, controlled trials. *Ann Intern Med* **135:**149–164.

Yamaoka K, Tanigawara Y, Nakagawa T, and Uno T (1981) A pharmacokinetic analysis program (multi) for microcomputer. *J Pharmacobiodyn* **4:**879–885.

Yedgar S, Carew TE, Pittman RC, Beltz WF, and Steinberg D (1983) Tissue sites of catabolism of albumin in rabbits. *Am J Physiol* **244:**E101–E107.

Address correspondence to: Dr. Masaki Otagiri, Department of Biopharmaceutics, Graduate School of Pharmaceutical Sciences, Kumamoto University, 5-1 Oe-honmachi, Kumamoto 862-0973, Japan. E-mail: otagirim@gpo.kumamoto-u.ac.jp

Nitric Oxide 22 (2010) 259–265

Contents lists available at ScienceDirect

Nitric Oxide

journal homepage: www.elsevier.com/locate/yniox

Nitrosylated human serum albumin (SNO-HSA) induces apoptosis in tumor cells ☆

Naohisa Katayama [a,b], Keisuke Nakajou [b], Yu Ishima [a], Shotaro Ikuta [b], Jun-ichi Yokoe [b], Fumika Yoshida [a], Ayaka Suenaga [a], Toru Maruyama [a,c], Toshiya Kai [a,b], Masaki Otagiri [a,d,*]

[a] Department of Biopharmaceutics, Graduate School of Pharmaceutical Sciences, Kumamoto University, 5-1 Oe-honmachi, Kumamoto 862-0973, Japan
[b] Pharmaceutical Research Center, Nipro 3023 Nojicho, Kusatsu, Shiga 525-0055, Japan
[c] Department of Clinical Pharmaceutics, Graduate School of Sciences, Kumamoto University, 5-1 Oe-honmachi, Kumamoto 862-0973, Japan
[d] Faculty of Pharmaceutical Sciences, Sojo University, 4-22-1 Ikeda, Kumamoto 860-0082, Japan

ARTICLE INFO

Article history:
Received 27 June 2009
Revised 19 September 2009
Available online 8 October 2009

Keywords:
SNO-HSA
Nitric oxide
Apoptosis
Anti-tumor effect
Cancer
Nitrosylation

ABSTRACT

Recently, nitric oxide has been investigated as a potential anti-cancer therapy because of its cytotoxic activity. Previously, we found that S-nitrosylated human serum albumin (SNO-HSA) induced apoptosis in C26 cells, demonstrating for the first time that SNO-HSA has potential as an anti-cancer drug. In the present study, the anti-tumor activity of SNO-HSA in another tumor type of cancer cell was investigated using murine tumor LY-80 cells. Mitochondrial depolarization, activation of caspase-3 and DNA fragmentation were induced in LY-80 cells by SNO-HSA treatment in a dose-dependent manner. Inhibition of caspase activity resulted in complete inhibition of DNA fragmentation induced by SNO-HSA. The cytotoxic effects of SNO-HSA on LY-80 were concentration-dependent. Tumor growth in LY-80-tumor-bearing rats was significantly inhibited by administration of SNO-HSA compared with saline- and HSA-treatment. These results suggest that SNO-HSA has potential as a chemopreventive and/or chemotherapeutic agent because it induces apoptosis in tumor cells.

© 2009 Elsevier Inc. All rights reserved.

Introduction

Somatic cells are generated by mitosis and almost all will die by apoptosis-physiologic cell suicide. Malignant growth occurs when this balance is disturbed due to either an increase in cellular proliferation or a decrease in cell death. There is a growing awareness that many of the changes that contribute to the development of cancers also interfere with apoptosis [1]. Therefore, induction of apoptosis in neoplastic cells effectively results in tumor eradication [2]. However, this type of chemotherapy often has negative side effects, such as transient cell cycle arrest, senescence, and autophagy. Drug delivery systems that facilitate selective apoptosis of neoplastic cells have been suggested as a way to overcome this problem [3,4].

Nitric oxide (NO)[1] is a unique, diffusible molecular messenger that plays a central role in mammalian pathophysiology [5]. The effects of NO are pleiotropic: vascular smooth muscle relaxation [6,7], inhibition of platelet aggregation [8], effects on neurotransmission [9], and regulation of immune function [10]. However, under some circumstances, NO is cytotoxic [11]. In L10 hepatoma cells, NO causes cellular iron loss, and inhibits DNA synthesis, mitochondrial respiration, and aconitase activity [12]. In addition, NO reacts with superoxide anion (which is produced by activated macrophages and other cells) to form peroxynitrite. This byproduct of NO is a potent chemical oxidant, which alters protein function and damages DNA [13]. These effects are part of the nonspecific host defense system, which facilitates killing of tumor cells and intracellular pathogens. In addition, the cytotoxic effects of long-lived NO result from induction of apoptosis [5]. In particular, high concentrations of NO inhibit tumor cell growth and induce apoptosis [14]. However, the half-life of NO *in vivo* (~0.1 s) is so short that NO itself cannot be used as a therapeutic agent. Recently, NO-donating non-steroidal anti-inflammatory drugs (NO-NSAIDs), in particular NO-aspirin (NO-ASA), have been investigated as promising chemopreventive agents [15–17]. NO-ASA consists of traditional ASA to which a NO-releasing moiety is bound via a spacer.

Previously, we selected human serum albumin (HSA) as the NO-carrier. S-nitrosylated HSA appears to act as a reservoir of NO *in vivo* [18] and, therefore, is expected to be a clinically feasible biocompatible pharmacological agent. One molecule of HSA contains 35 cysteine residues. However 34 of them form 17 non-reactive disulfide bonds, and thus only one residue (Cys-34) forms a reactive free thiol for S-nitrosylation [19]. Consequently, we increased the number of free sulfhydryl groups on HSA. HSA was reacted with

☆ SNO-HSA induces apoptosis in tumor cells.

* Corresponding author. Fax: +81 96 362 7690.
E-mail address: otagirim@gpo.kumamoto-u.ac.jp (M. Otagiri).

[1] *Abbreviations:* NO, nitric oxide; SNO-HSA, nitrosylated human serum albumin; rHSA, recombinant human serum albumin; NO-NSAID, nitric oxide-donating non-steroidal anti-inflammatory drug; NO-ASA, nitric oxide-donating aspirin; DTPA, diethylenetriaminepentaacetic acid; LDH, lactate dehydrogenase; BSA, bovine serum albumin; R410C, genetic variant of human serum albumin mutated at position 410.

1089-8603/$ - see front matter © 2009 Elsevier Inc. All rights reserved.
doi:10.1016/j.niox.2009.09.003

iminothiolane to produce poly S-nitrosylated HSA (SNO-HSA, 6.6 mol SNO/mol HSA). SNO-HSA induced oxidative stress and apoptosis via activation of the intrinsic apoptosis pathway in murine colon 26 carcinoma (C26) cells *in vitro*. Furthermore, intravenous administration of SNO-HSA inhibited tumor growth in C26 tumor-bearing mice, due to its pro-apoptosis effects [20].

In the present study, the anti-tumor activity of SNO-HSA was evaluated extensively using a rat tumor cell line-LY-80 (a variant of Yoshida sarcoma). The LY-80 cell line is a non-adherent cell type that can be implanted into the rat; thus LY-80 cells have been utilized for cancer research. The molecular events by which SNO-HSA induces apoptosis were studied *in vitro* and the anti-tumor activity of SNO-HSA was studied *in vivo* using a rat model of LY-80 sarcoma.

Materials and methods

Chemicals

Traut's Reagent (2-imminothiolane) was purchased from Pierce Chemical Co. (Rockford, IL, USA). Isopentyl nitrite, diethylenetriaminepentaacetic acid (DTPA) and a Cell Counting Kit-8 were purchased from Wako Pure Chemical Industries, Ltd. (Osaka, Japan). RPMI-1640 medium and RNase A were obtained from Sigma Chemical (St. Louis, MO, USA). Proteinase K was obtained from Roche Applied Science (Indianapolis, IN, USA). All other reagents were the highest grade available from commercial sources.

Expression and purification of recombinant human serum albumin (rHSA)

rHSA was produced using a yeast expression system as described previously [21]. Briefly, to construct the HSA expression vector, pPIC9-HSA, a native HSA coding region was incorporated into the methanol-inducible pPIC9 vector (Invitrogen Co., San Diego, CA, USA). The resulting vector was introduced into the yeast species, *P. pastoris* (strain GS115), for expression of rHSA. Secreted rHSA was isolated from the growth medium by both precipitation with 60% (w/v) $(NH_4)_2SO_4$ and purification on a Blue Sepharose CL-6B column (GE Healthcare, Buckinghamshire, England) and then on a Phenyl HP column (GE Healthcare, Buckinghamshire, England). The isolated protein was defatted using the charcoal procedure described by Chen [22], deionized, freeze-dried and then stored at −20 °C until use. The resulting rHSA (treated with dithiothreitol) exhibited a single band on SDS/PAGE. Density analysis of protein bands stained with Coomassie brilliant blue revealed the final produce was ⩾97% pure.

Synthesis of HSA (I), SNO-HSA and SNO-HSA (R)

Terminal sulfhydryl groups were added to the HSA molecule by incubation of 0.15 mM rHSA with 3 mM Traut's Reagent (2-imminothiolane) in 100 mM potassium phosphate buffer containing 0.5 mM DTPA (pH 7.8) for 1 h at room temperature. The resultant modified rHSA then was divided into two portions, after that one was concentrated, exchanged with saline and adjusted to 2 mM, designated as HSA (I), the other was S-nitrosylated via 3 h incubation with 15 mM isopentyl nitrite at room temperature. The resulting SNO-HSA was concentrated and exchanged with saline using a PelliconXL filtration device (Millipore Corporation, Billerica, MA, USA). The final concentration was adjusted to 2 mM SNO-HSA and the sample was stored at −80 °C until use.

In order to obtain free sulfhydryl groups on HSA molecule, 0.3 mM HSA was incubated with 30 mM dithiothreitol in 200 mM Tris–HCl buffer containing 1 mM EDTA and 8 M urea (pH 8.2) for 4 h at room temperature. Dithiothreitol was then quickly removed by Sephadex G-25 gel filtration and eluted with 100 mM acetic acids. Then, 0.1 mM reduced HSA was incubated with 10 mM isoamyl nitrite in 100 mM potassium phosphate buffer containing 0.5 mM DTPA (pH 7.8) for 1 h at room temperature, followed by Sephadex G-25 gel filtration, concentration and exchange with saline to 2 mM SNO-HSA (R). The sample was stored at −80 °C until use.

The number of the S-nitroso moieties on SNO-HSA and SNO-HSA (R) were determined using a 96-well plate. First, 20-μl aliquots of sample solutions and $NaNO_2$ (standard) were incubated with 0.2 ml of 10 mM sodium acetate buffer (pH 5.5) containing 100 mM NaCl, 0.5 mM DTPA, 0.015% N-1-naphthylsthylene-diamide and 0.15% sulfanilamide with or without 0.09 mM $HgCl_2$ for 30 min at room temperature. Then, absorbance at 540 nm was measured. The number of moles of NO per mole of HSA was estimated by subtracting the values obtained in the absence of $HgCl_2$ from those measured in the presence of $HgCl_2$; the values obtained from SNO-HSA and SNO-HSA (R) were 6.6 ± 0.5 and 3.3 ± 0.6 mol NO/mol HSA, respectively [23].

Cellular experiments with LY-80 cells

LY-80 Yoshida sarcoma cells (non-adherent cell), which were donated by the Institute of Development, Aging and Cancer, at Tohoku University (Sendai, Miyagi, Japan), were cultured at 37 °C in RPMI-1640 medium containing 10% fetal calf serum, 100 U/ml penicillin, and 10 μg/ml streptomycin (medium A). All cell culture experiments were performed at 37 °C in a humidified atmosphere of 5% CO_2 in air.

Changes in the mitochondrial membrane potential of LY-80 cells were monitored using flow cytometric analysis with rhodamine 123-staining. LY-80 cells (1.0×10^6 cells/well) were cultured in 12-well plates with PBS, 50 μM HSA or the indicated concentrations of SNO-HSA for 2 h. The cells then were incubated for 15 min with 10 μM rhodamine 123, followed by centrifugation at 4000 rpm for 5 min. The cell pellet was resuspended in 0.3 ml of PBS and the fluorescence intensity of rhodamine 123 in the cells was measured using a flow cytometer (FACS Calibur; Becton Dickinson Biosciences, Franklin Lakes, USA).

Caspase-3 activity was determined as follows. Cells (1.0×10^6 cells/well) were incubated in 6-well plates with medium A containing PBS, 100 μM HSA, HSA (I), SNO-HSA (R) or various concentrations of SNO-HSA. After incubation for 24 h, the cells were collected by centrifugation at 4000 rpm for 10 min and the cell pellet was washed with 0.2 ml of ice-cold PBS, followed by centrifugation. The cell pellet was resuspended in 10 μl of cell-lysis buffer. The cells were then lysed by freeze thawing, followed by a 15-min incubation on ice. The cell lysates were centrifuged at 15,000 rpm for 20 min at 4 °C, and the supernatant fraction was collected (cell extract). The caspase-3 activity in the cell extract was assessed using the colorimetric CaspASE™ Assay System (Promega, Tokyo, Japan), according to the manufacturer's instructions.

DNA degradation (DNA ladder) was detected as follows. LY-80 cells (1×10^6 cell/well) were cultured in 12-well plates with PBS, 100 μM HSA or the indicated concentrations of SNO-HSA. After incubation, culture medium containing the cells was collected and centrifuged at 4000 rpm for 5 min. After removal of the supernatant, the cell pellet was resuspended in 0.2 ml of PBS and centrifuged at 4000 rpm for 10 min. The resulting pellet was incubated in 20 μl of 10 mM Tris–HCl buffer (pH 7.8) containing 2 mM EDTA and 0.5% SDS for 10 min at 4 °C, followed by centrifugation at 15,000 rpm for 5 min. The resulting supernatant (cell extract) was collected and incubated with 1 μl of RNase A (10 μg/ml) for 30 min at 50 °C. One microliter of proteinase K (10 μg/ml) was added to the cell extract, followed by a 1-h incubation at 50 °C.

The resulting DNA extract was electrophoresed in a 2.0% agarose gel, followed by staining of the gel with ethidium bromide and visualization of the DNA bands using ultraviolet illumination.

For inhibition assays, LY-80 cells were incubated for 12 h with 100 μM SNO-HSA in the absence or presence of 50 μM Z-VAD-FMK (caspase inhibitor). The extent of DNA fragmentation was determined as described above.

Cell proliferation was quantified using a Cell Counting Kit-8 (WST-8), which is based on the MTT assay. LY-80 cells were plated in 96-well plates at 1.0×10^4 cells/well and incubated for 48 h in a total volume of 0.2 ml medium A containing various concentrations of HSA or SNO-HSA. After incubation, 5 μl of WST-8 solution was added to each well and the cells were incubated for an additional 2 h at 37 °C. The number of surviving cells was determined by measurement of absorbance at 450 nm. Cell viability was calculated as a percentage of the control culture (without either HSA or SNO-HSA) [24].

For determination of lactate dehydrogenase (LDH) activity, LY-80 cells (1.0×10^4 cells/well) were incubated in 96-well plates with the indicated concentrations of HSA or SNO-HSA. After incubation for the indicated times, culture medium containing the cells was collected and centrifuged at 4000 rpm for 10 min. LDH activity in the supernatant was assessed using the LDH-Cytotoxicity Assay Kit (Bio Vision), according to the manufacturer's instructions. Cytotoxicity was calculated as a percentage based on the LDH activity released from cells that had been treated with compound compared with LDH activity from cultures incubated with Triton.

Animal experiments

Five-week-old, male Donryu rats (200–250 g) were purchased from Charles River (Nippon Charles-River Co., Ltd., Shizuoka, Japan). The rats were housed under a 12/12 h light/dark cycle in a humidity-controlled room. The rats were acclimated for at least 5 days prior to use in the experiments.

LY-80 cells (2×10^6 cells) that had been sub-cultured in the abdominal cavity of a Donryu rat were implanted in the right thigh of the experimental rats. Five days after inoculation, LY-80 sarcoma-bearing rats were randomly assigned to three groups: control (saline), HSA, and SNO-HSA. The rats received either a daily intravenous or direct intra-tumor injection of saline, HSA (10 μmol/kg), or SNO-HSA (10 μmol/kg), for 7 days (day 5–11 post-inoculation). Tumor volume was calculated using the formula 0.4 ($a \times b^2$), where 'a' is the largest and 'b' is the smallest tumor diameter [25]. Data are expressed as means ± SD. Differences between groups were evaluated using the paired Student's t-test. A p-value of less than 5% was considered to indicate a statistically significant difference.

Results

SNO-HSA induces cell death via apoptosis in vitro

Mitochondria play a pivotal role in the regulation of mammalian apoptosis, which is believed to result from loss of mitochondrial membrane potential. To evaluate the effects of SNO-HSA on mitochondrial function and membrane potential, LY-80 cells were loaded with a mitochondrion-selective fluorescent cation (rhodamine 123). Compared with vehicle (PBS), SNO-HSA treatment decreased rhodamine fluorescent intensity in a dose-dependent manner. HSA also attenuated fluorescence, but to a lesser extent than SNO-HSA (Fig. 1). This observation indicates that SNO-HSA induces depolarization of the mitochondrial membrane.

Caspase-3 is a cell-death protease that is involved in the downstream execution phase of apoptosis, during which cells undergo

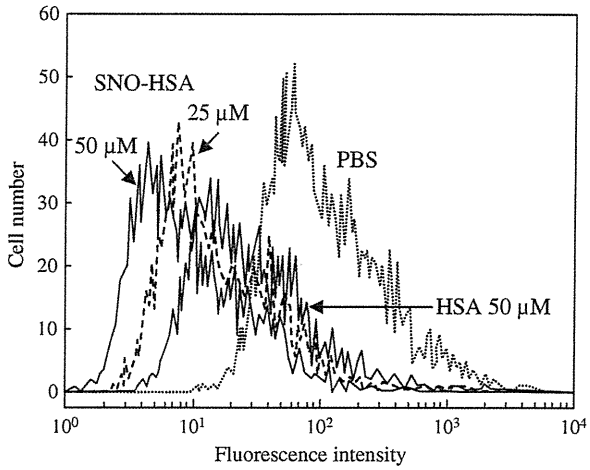

Fig. 1. Mitochondrial transmembrane potential is altered by SNO-HSA treatment. LY-80 cells were cultured with either PBS, 50 μM HSA, or various concentrations of SNO-HSA for 2 h, followed by addition of rhodamine 123. Mitochondrial transmembrane potential was analyzed using flow cytometry. Results are shown for one representative experiment.

morphological changes, such as DNA fragmentation, chromatin condensation, and formation of apoptotic bodies. Compared with vehicle-treated cultures, cells treated with 25, 50 or 100 μM SNO-HSA showed relative increases in caspase-3 activity of 21-, 34- and 42-fold, respectively. The caspase-3 activity of HSA-treated cells was equivalent to that of cells treated with PBS. In addition, in order to elucidate the effect of iminothiolane on the activation of caspase-3, HSA (I) and SNO-HSA (R) were also incubated with LY-80 cells. Surprisingly, SNO-HSA (R) as well as HSA (I) did not activate caspase-3, which suggested that iminothiolane did not participate in the activation of caspase-3 and that NO bound via functional thiols introduced by reaction of iminothiolane with terminal amines in HSA might be more efficient for its release than NO bound to terminal thiols obtained by reduction (Fig. 2). As an interesting observation supporting the result, uptake of NO from

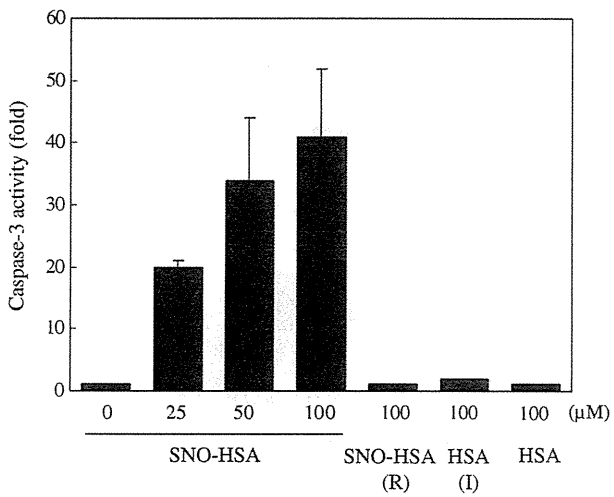

Fig. 2. Activation of caspase-3 after SNO-HSA treatment. LY-80 cells were incubated with either PBS, 100 μM HSA, HSA (I), SNO-HSA (R) or various concentrations of SNO-HSA for 24 h. Because the amounts of NO bound to SNO-HSA (R) and SNO-HSA are 6.6 ± 0.5 and 3.3 ± 0.6 mol NO/mol HSA, respectively, NO content of SNO-HSA (R) is nearly equivalent to 50 μM SNO-HSA. Caspase-3 activity was determined as described in Material and methods and is expressed as the ratio of absorbance estimated from the culture with the test compound relative to the absorbance of cultures incubated with PBS. Results are means ± SD of three separate experiments.

SNO-HSA to HepG2 cell was much higher than that from SNO-HSA (R) (our unpublished observations). The mechanisms by which the difference of NO uptake between SNO-HSA and SNO-HSA (R) arose need to be investigated in future studies.

To further confirm that SNO-HSA induced apoptosis in LY-80 cells, DNA fragmentation, which is a morphological change characteristic of the execution phase of apoptosis, was examined. DNA fragmentation was observed in LY-80 cells after 4 h of incubation in 100 μM SNO-HSA and stabilized after 8 h. However, DNA fragmentation was not detected until 24 h of incubation in 100 μM HSA (Fig. 3A). Moreover, the DNA ladder observed after 12 h of incubation in SNO-HSA increased in a dose-dependent manner (Fig. 3B). To determine the mechanism by which SNO-HSA causes DNA fragmentation, LY-80 cells were simultaneously incubated with SNO-HSA and Z-VAD-FMK (a caspase inhibitor). DNA fragmentation induced by 100 μM SNO-HSA was completely abolished by treatment with Z-VAD-FMK (Fig. 3C). This result indicates that caspases are positive, upstream regulators of the DNA fragmentation that is elicited by SNO-HSA.

To determine the effect of SNO-HSA on cell growth, the viability of LY-80 cells was examined after treatment with either HSA or various concentrations of SNO-HSA. SNO-HSA inhibited growth of LY-80 cells in a concentration-dependent manner. HSA also tended to abrogate cell proliferation, but to a lesser extent than SNO-HSA (Fig. 4).

To further characterize SNO-HSA-induced LY-80 cell death, cytotoxicity was examined using an assay of LDH activity. LDH is a stable enzyme that is rapidly released from cells into the cell culture medium upon damage to the plasma membrane. Cell death increased with incubation duration for the cultures incubated with

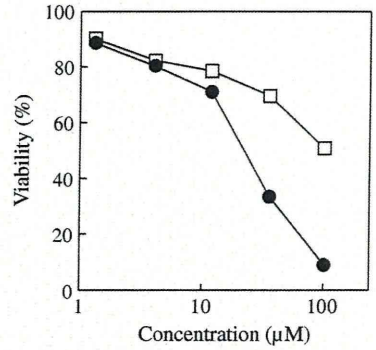

Fig. 4. Effect of SNO-HSA on cell viability. LY-80 cells were treated for 48 h with various concentrations of HSA (open squares) or SNO-HSA (closed circles). Cell viability was determined as described in Materials and methods. Results from three separate experiments are presented as means.

100 μM SNO-HSA. After 48 h of incubation, LDH was released from nearly all cells. In contrast, HSA was not cytotoxic (Fig. 5A). Furthermore, SNO-HSA was cytotoxic to LY-80 cells in a dose-dependent manner (Fig. 5B). These results suggest that SNO-HSA induced cell death via activation of an intrinsic apoptosis-signaling pathway.

SNO-HSA exerts anti-tumor effects in vivo

To investigate the anti-tumor effects of SNO-HSA *in vivo*, LY-80 tumor-bearing rats received either intravenous or direct intra-tumor injections of either saline, HSA or SNO-HSA. These treatments

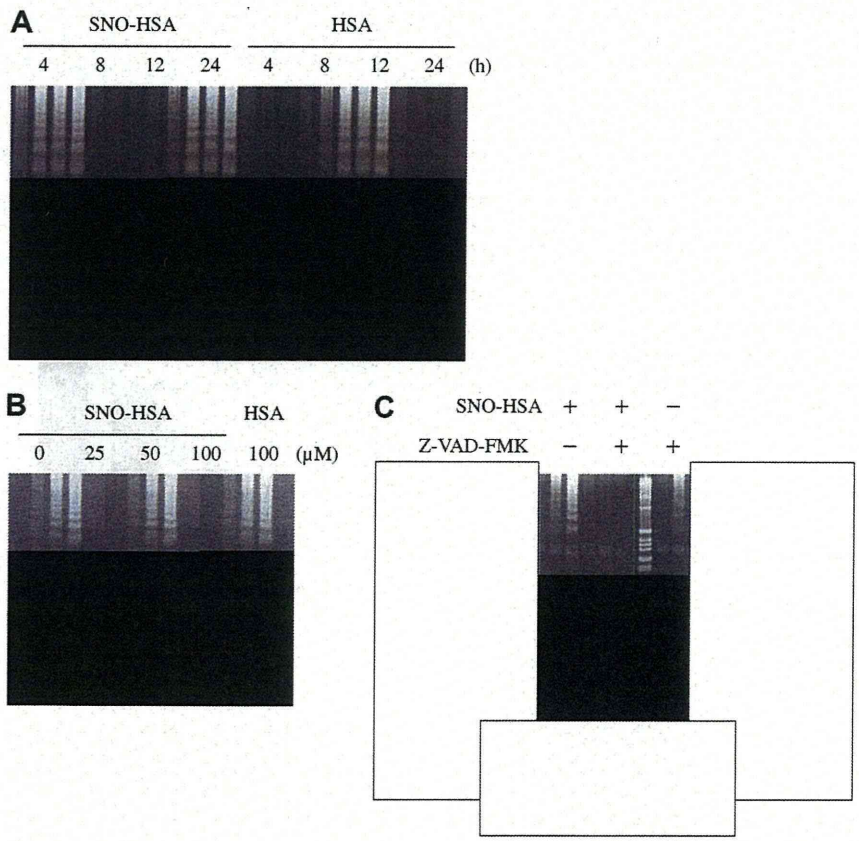

Fig. 3. DNA fragmentation after SNO-HSA treatment. (A) LY-80 cells were incubated for the indicated times with 100 μM HSA or SNO-HSA. (B) LY-80 cells were incubated for 12 h with 100 μM HSA or the indicated concentrations of SNO-HSA. (C) LY-80 cells were incubated for 12 h with 100 μM SNO-HSA in the presence or absence of 50 μM Z-VAD-FMK (caspase inhibitor). DNA fragmentation was detected as described in Materials and methods.

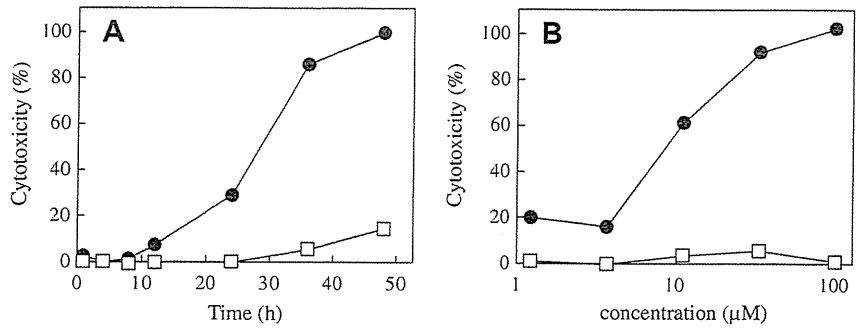

Fig. 5. Effect of SNO-HSA on LDH release (cytotoxicity). (A) LY-80 cells were incubated for the indicated times with 100 μM HSA (open squares) or SNO-HSA (closed circles). (B) LY-80 cells were treated for 48 h with various concentrations of HSA (open squares) or SNO-HSA (closed circles). LDH released from the cells was quantified as described in Materials and methods. Cytotoxicity was plotted as a percentage of total LDH release. Results from three separate experiments are presented as means.

were repeated daily for seven days (day 5–11 post-inoculation). Mean tumor volume increased with time in the saline-treated group. A similar result was also observed in the HSA-treated group. However, tumor growth in animals that received direct intra-tumor injections of SNO-HSA was only one-third that observed in the saline- and HSA-treated animals (Fig. 6). This observation suggests that SNO-HSA has anti-tumor effects *in vivo*, presumably due to induction of apoptosis. In contrast, the effects of intravenous injection of SNO-HSA on tumor growth were not significantly different from those observed with saline- and HSA-treatment (data not shown).

Discussion

We have previously reported that SNO-HSA induces intracellular changes that are characteristic of apoptosis, including mitochondrial depolarization, activation of caspase-3 and DNA fragmentation in C26 cells. In addition, intravenous injection of SNO-HSA into C26 cell-bearing mice suppressed tumor growth due to activation of the apoptotic pathway. The purpose of the present study was to evaluate the effects of SNO-HSA on a different carcinoma cell line, LY-80 cells, and to further characterize the mechanism by which SNO-HSA induces apoptosis. In the present study, SNO-HSA also elicited mitochondrial depolarization (Fig. 1), activated caspase-3 (Fig. 2) and induced DNA fragmentation (Fig. 3) in LY-80 cells. Inhibition of caspases by co-incubation with Z-VAD-FMK completely inhibited DNA fragmentation (Fig. 3C). This observation suggests that caspase activation is essential for induction of apoptosis by SNO-HSA and that these molecular events result in cell death (Figs. 4 and 5). Furthermore, injection of SNO-HSA directly into tumor tissue inhibited tumor growth in LY-80 tumor-bearing rats *in vivo*. Therefore, SNO-HSA has anti-tumor activity against LY-80 cancer cells, as well as against C26 cells.

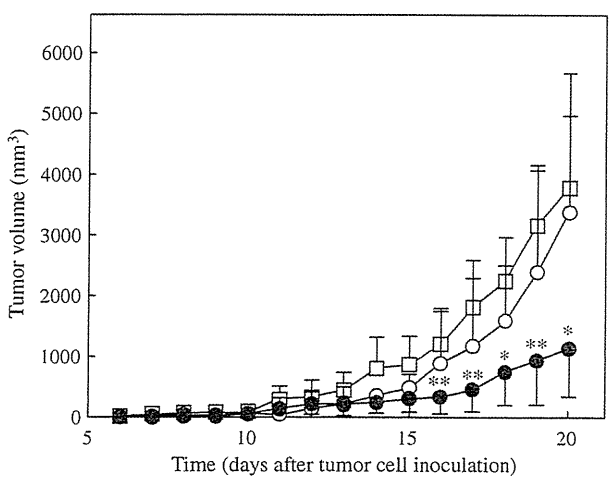

Fig. 6. Effect of SNO-HSA on tumor growth in LY-80 tumor-bearing rats. LY-80 tumor-bearing rats were given daily intra-tumor injections of saline (5 ml/kg; open squares), HSA (10 μmol/5 ml/kg; open circles) or SNO-HSA (10 μmol/5 ml/kg; closed circles) for 7 days (day 5–11 after inoculation with tumor cells). Tumor size was measured and tumor volume was calculated according to the formula: $V = 0.4a^2b$, where a is the smallest, and b the largest, superficial diameter. Results are means ± SD; $n = 4$ animals per experimental group. *Statistically significant reduction compared with saline- ($P < 0.01$) or HSA- ($P < 0.01$) treatment at the corresponding time. **Statistically significant reduction compared with saline- ($P < 0.01$) or HSA- ($P < 0.05$) treatment groups at the corresponding time.

However, *in vivo*, the effects of SNO-HSA on LY-80 cells differed from those observed for C26 cells. In the present study, direct intra-tumor injections of SNO-HSA into LY-80 tumor-bearing rats suppressed tumor growth, possibly due to induction of apoptosis. Unexpectedly, intravenous injection of SNO-HSA did not have an anti-tumor effect (data not shown). In contrast, we previously reported that tumor growth in C26 tumor-bearing mice was significantly inhibited by intravenous administration of SNO-HSA. One possible reason for the inconsistent results is that tumor blood flow might be reduced in LY-80 tumor-bearing rats compared with that in animal models of other cancers, including C26 tumor-bearing mice. Tanda et al. evaluated tumor growth in LY-80 tumor-bearing rats after intravenous administration of adriamycin (ADM) with or without dopamine (DA), which increased tumor blood flow. Despite ADM has potent anti-tumor effects of ADM, administration of ADM alone did not affect the growth of the LY-80 tumor. However, co-administration of ADM and DA inhibited tumor growth. This result suggests that delivery of substances injected intravenously is in inefficient because tumor blood flow is attenuated in LY-80 tumor-bearing rats [26]. Similarly, intravenous injection of SNO-HSA into LY-80 tumor-bearing mice might limit the anti-tumor effects of SNO-HSA. In contrast, Ogawara et al. examined the anti-tumor effects of polyethylene glycol (PEG)-modified liposomal doxorubicin (DOX) in three different tumor cell lines (Lewis lung cancer (LLC), C26 and B16BL6 melanoma (B16)) *in vitro* and *in vivo*. Although LLC exhibited the greatest sensitivity to DOX *in vitro*, the strongest *in vivo* anti-tumor effect was observed in the C26 tumor-bearing mice. Evans blue extravasation and secretion of VEGF in C26 tumors were greater than in LLC tumors [27]. These findings suggest that the vasculature in C26 tumors was more permeable than that of other tumor cell lines. Therefore, the difference in vascular permeability between LY-80

and C26 tumors may be a major cause of the different response to intravenous administration of SNO-HSA. Another possible explanation is the rapid clearance of SNO-HSA *in vivo*. In our previous report, intravenous injection of SNO-HSA significantly inhibited tumor growth in C26 tumor-bearing mice, but daily injections were required to elicit a therapeutic effect. SNO-HSA is considered to be a reservoir of NO *in vivo*. HSA is the most abundant protein in plasma and it has a longer half-life than other NO donors. However, the apparent *in vivo* half-life of the S-nitroso moieties on SNO-HSA was estimated to be 18.9 min (data not shown); HSA-bound compounds are not always long-acting therapeutic agents. Therefore, rapid elimination of SNO-HSA may also explain the lack of *in vivo* activity following intravenous injection. In this context, Katsumi et al. prepared poly-NO-BSA conjugated with polyethylene glycol (PEG) and showed that, *in vitro*, the half-life of NO was 11 times longer than that of poly-NO-BSA without PEG [28]. Consequently, modification with PEG may enhance the anti-tumor activity of SNO-HSA. Furthermore, HSA molecules tend to accumulate in tumor tissues, apparently due to hypervascularization and enhanced vascular permeability (even to macromolecules) of the tumor, and minimal export of macromolecules from the tumor tissue via blood or lymphatic vessels [29]. Therefore, it was expected that SNO-HSA would enhance NO accumulation in tumors and, therefore, would be a useful agent for targeting chemotherapeutics to tumors.

In both the present study and our earlier investigation, HSA alone decreased the viability of both LY-80 cells (Fig. 4) and C26 cells compared with control cultures that were incubated without additives. In the experiment shown in Fig. 4, WST-8 is bio-reduced by cellular dehydrogenase in viable cells to produce an orange formazan product. The amount of the formazan product is directly proportional to the number of viable cells, but is not related to the ratio of living cells/total cells. Ten percent of FCS in medium A used in this experiment includes 4.1 mg/ml of proteins containing 3.3 mg/ml of albumin (~50 μM). Therefore, total amount of proteins in medium A containing 100 μM HSA reaches 10.8 mg/ml in which 10.0 mg/ml of albumin (~150 μM) is included, indicating that cells treated with 100 μM HSA are cultured at 2.6 times higher concentrations of proteins than control culture (calculated as 100% viability). Accordingly, the inhibition of cell proliferation by HSA might result from high concentrations of protein at which LY-80 cells are cultured. In contrast, in the experiment shown in Fig. 5, determination of LDH released by dead cells is indicative of the level of cellular cytotoxicity. Incubation with HSA did not result in LDH release (Fig. 5). Taken together, these observations suggest that HSA (or high concentrations of proteins) inhibits cell proliferation, but is not cytotoxic.

Although we assumed that NO plays a key role in SNO-HSA-induced apoptosis, there are many reports describing the anti-apoptotic effects of NO. The amount of NO may be one of the most potential causes for this discrepancy. The NO contents of SNO-HSA used in our studies were 6.6 mol NO/mol HSA and the S-nitroso moiety concentrations *in vitro* were 165–660 μM (25–100 μM as HSA molecule). Qiang et al. reported that high concentrations GSNO (100–300 μM) induced apoptosis and inhibited cell growth in colon cancer cell lines, such as HCA7, HT29 and HCT116 [14]. Mebmer et al. reported that apoptosis (characterized by DNA fragmentation and morphological changes) was observed in U937 cells treated with GSNO at concentrations in excess of 250 μM [30]. In contrast, NO-R410C (a genetic variant of HSA) had anti-apoptotic activity at 26–130 μM in U937 cells [31], and 10–100 μM GSNO inhibited actinomycin D-induced activation of caspase-3 in U937 cells [32]. Based on the results of the present study and those of previously published investigations, the critical NO concentration that determines if NO promotes or inhibits apoptosis appears to be 100–200 μM NO. On the other hand, SNO-HSA never inhibited the activation of caspase-3 at any concentration lower than 100 μM NO, because the activity of caspase-3 was originally little observed in LY-80 cells and thus it was difficult to detect its reduction. To resolve this issue, the effect of SNO-HSA might be needed to be investigated under conditions where caspase-3 is activated by appropriate substance.

In summary, the cytotoxic activity of NO is currently being investigated for use in anti-cancer therapies. The present study was undertaken to evaluate the anti-tumor activity of SNO-HSA in LY-80 tumor cells. SNO-HSA activated an intrinsic apoptosis-signaling pathway, resulting in cell death. In the *in vivo* experiments, direct intra-tumor injection of SNO-HSA inhibited tumor growth, while intravenous administration had no effect on tumor growth. Thus, SNO-HSA with a long half-life may be a promising candidate for cancer therapy. In addition, SNO-HSA is an endogenous substance and has few side effects, as reported previously.

References

[1] H. Okada, T.W. Mak, Pathways of apoptotic and non-apoptotic death in tumor cells, Nat. Rev. Cancer (4) (2004) 592–603.
[2] X.W. Meng, S.H. Lee, S.H. Kaufmann, Apoptosis in the treatment of cancer: a promise kept?, Curr Opin. Cell Biol. 18 (2006) 668–676.
[3] S.H. Kaufmann, G.J. Gores, Apoptosis in cancer: cause and cure, Bioessays 22 (2000) 1007–1017.
[4] Y. Kondo, T. Kanzawa, R. Sawaya, S. Kondo, The role of autophagy in cancer development and response to therapy, Nat. Rev. Cancer 5 (2005) 726–734.
[5] B. Brune, K. Sandau, A.V. Knethen, Apoptotic cell death and nitric oxide: activating and antagonistic transducing pathways, Biochemistry (Mosc.) 63 (1998) 817–825.
[6] S. Moncada, A. Higgs, The L-arginine–nitric oxide pathway, N. Engl. J. Med. 329 (1993) 2002–2012.
[7] L.J. Ignarro, Endothelium-derived nitric oxide – pharmacology and relationship to the actions of organic nitrate esters, Pharmacol. Res. 6 (1989) 651–659.
[8] H. Azuma, M. Ishikawa, S. Sekizaki, Endothelium-dependent inhibition of platelet aggregation, Br. J. Pharmacol. 88 (1986) 411–415.
[9] J. Garthweite, Glutamate, nitric oxide and cell–cell signaling in the nervous system, Trends Neurosci. 14 (1991) 60–67.
[10] M.A. Marletta, P.S. Yoon, R. Iyengar, C.D. Leaf, J.S. Wishnok, Macrophage oxidation of L-arginine to nitrite and nitrate–nitric oxide is an intermediate, Biochemistry 27 (1988) 8706–8711.
[11] F. Laval, D.A. Wink, Inhibition by nitric oxide of the repair protein, O6-methylguanine-DNA-methyltransferase, Carcinogenesis 15 (1994) 443–447.
[12] J.B. Hibbs Jr., R.R. Taintor, Z. Vavrin, E.M. Rachlin, Nitric oxide: a cytotoxic activated macrophage effector molecule, Biochem. Biophys. Res. Commun. 157 (1988) 87–94.
[13] J.S. Beckman, J.P. Crow, Pathological implication of nitric oxide, superoxide and peroxnitrite formation, Biochem. Soc. Trans. 21 (1993) 330–334.
[14] L. Qiang, S.T.F. Chan, R. Mahendran, Nitric oxide induces cyclooxygenase expression and inhibits cell growth in colon cancer cell lines, Carcinogenesis 24 (2003) 637–642.
[15] F. Fabbri, G. Brigliadori, P. Ulivi, A. Tesei, I. Vannini, M. Rosetti, S. Bravaccini, D. Amadori, M. Bolla, W. Zoli, Pro-apoptotic effect of a nitric oxide-donating NSAID, NCX4040, on bladder carcinoma cells, Apoptosis 10 (2005) 1095–1103.
[16] K. Kashifi, Y. Ryann, L.L. Qiao, J.L. Williams, J. Chen, P.D. Soldato, F.T. Traganos, B. Rigas, Nitric oxide-donating nonsteroidal anti-inflammatory drugs inhibit the growth of various cultured human cancer cells: evidence of a tissue type-independent effect, J. Pharmacol. Exp. Ther. 303 (2002) 1273–1282.
[17] J.L. Williams, S. Borgo, I. Hasan, E. Castillo, F. Traganos, B. Rigas, Nitric oxide-releasing nonsteroidal anti-inflammatory drugs (NSAIDs) alter the kinetics of human colon cancer cell lines more effectively than traditional NSAIDs: implication for colon cancer chemoprevention, Cancer Res. 61 (2001) 3285–3289.
[18] J.S. Stamler, O. Jaraki, J. Osborne, D.I. Simon, J. Keaney, J. Vita, D. Singel, C.R. Valeri, J. Loscalzo, Nitric oxide circulates in mammalian plasma primarily as an S-nitroso adduct of serum albumin, Proc. Natl. Acad. Sci. USA 89 (1992) 7674–7677.
[19] T. Peters Jr., Serum albumin, Adv. Protein Chem. 37 (1985) 161–245.
[20] N. Katayama, K. Nakajou, H. Komori, K. Uchida, J.I. Yokoe, N. Yasui, H. Yamamoto, T. Kai, M. Sato, T. Nakagawa, M. Takeya, T. Maruyama, M. Otagiri, Design and evaluation of S-nitrosylated human serum albumin as a novel anticancer drug, J. Pharmacol. Exp. Ther. 325 (2008) 69–76.
[21] S. Matsushita, Y. Ishima, V.T. Chuang, H. Watanabe, S. Tanase, T. Maruyama, M. Otagiri, Functional analysis of recombinant human serum albumin domains for pharmaceutical applications, Pharm. Res. 10 (2004) 1924–1932.
[22] R.F. Chen, Removal of fatty acids from serum albumin by charcoal treatment, J. Biol. Chem. 242 (1967) 173–181.
[23] A.F. Habeeb, Determination of free amino groups in proteins by trinitrobenzene–sulfonic acid, Anal. Biochem. 14 (1966) 328–336.
[24] M. Ishiyama, H. Tominaga, M. Shiga, K. Sasamoto, Y. Ohkura, K. Ueno, A combined assay of cell viability and in vitro cytotoxicity with a highly water-

soluble tetrazolium salt, neutral red and crystal violet, Biol. Pharm. Bull. 19 (1996) 1518–1520.
[25] K. Shimizu, T. Asai, C. Fuse, Y. Sadzuka, T. Sonobe, K. Ogino, T. Taki, T. Tanaka, N. Oku, Applicability of anti-neovascular therapy to drug-resistant tumor: suppression of drug-resistant P388 tumor growth with neovessel-targeted liposomal adriamycin, Int. J. Pharm. 296 (2005) 133–141.
[26] S. Tanda, K. Hori, Q.H. Zhang, H.C. Li, M. Suzuki, Effects of intravenous infusion of dopamine on tumor blood flow in rats subcutis, Jpn. Cancer Res. 85 (1994) 556–562.
[27] K.I. Ogawara, K. Un, K. Minato, K.I. Tanaka, K. Higaki, T. Kimura, Determinants for in vivo anti-tumor effects of PEG liposomal doxorubicin: importance of vascular permeability within tumors, Int. J. Pharm. 359 (2008) 234–240.
[28] H. Katsumi, M. Nishikawa, F. Yamashita, M. Hashida, Development of polyethylene glycol-conjugated poly-s-nitrosated serum albumin, a novel s-nitrosothiol for prolonged delivery of nitric oxide in the blood circulation in vivo, J. Pharmacol. Exp. Ther. 314 (2005) 1117–1124.
[29] Y. Matsumura, T. Oda, H. Maeda, General mechanism of intratumor accumulation of macromolecules: advantage of macromolecular therapeutics, Jpn. J. Cancer Chemother. 14 (pt. II) (1987) 821–829.
[30] U.K. Mebmer, D.M. Reimer, B. Brune, Nitric oxide-induced apoptosis: p53-dependent and p53-independent signaling pathways, Biochem. J. 319 (1995) 299–305.
[31] Y. Ishima, T. Sawa, U. Kragh-Hansen, Y. Miyamoto, S. Matsushita, T. Akaike, M. Otagiri, S-nitrosylation of human variant albumin Liprizzi (R410C) confers potent antibacterial and cytoprotective properties, J. Pharmacol. Exp. Ther. 320 (2007) 969–977.
[32] S. Mohr, B. Zech, E.G. Lapetina, B. Brune, Inhibition of caspase-3 by S-nitrosation and oxidation caused by nitric oxide, Biochem. Biophys. Res. Commun. 238 (1997) 387–391.

Nitric Oxide 23 (2010) 121–127

Contents lists available at ScienceDirect

Nitric Oxide

journal homepage: www.elsevier.com/locate/yniox

One-step preparation of *S*-nitrosated human serum albumin with high biological activities

Yu Ishima [a,1], Shuichi Hiroyama [a,1], Ulrich Kragh-Hansen [b], Toru Maruyama [a], Tomohiro Sawa [c], Takaaki Akaike [c], Toshiya Kai [a,d], Masaki Otagiri [a,e,*]

[a] *Department of Biopharmaceutics, Graduate School of Pharmaceutical Sciences, Kumamoto University, 5-1 Oe-honmachi, Kumamoto 862-0973, Japan*
[b] *Department of Medical Biochemistry, University of Aarhus, DK-8000 Aarhus C, Denmark*
[c] *Department of Microbiology, Graduate School of Medical Sciences, Kumamoto University, 1-1-1 Honjo, Kumamoto 860-0811, Japan*
[d] *Pharmaceutical Research Center, Nipro, 3023 Nojicho, Kusatsu, Shiga 525-0055, Japan*
[e] *Faculty of Pharmaceutical Sciences, Sojo University, 4-22-1 Ikeda, Kumamoto 860-0082, Japan*

ARTICLE INFO

Article history:
Received 5 February 2010
Revised 28 April 2010
Available online 6 May 2010

Keywords:
Human serum albumin
Nitric oxide
N-Acetyl-L-tryptophan
Caprylic acid
S-Nitrosation
Ischemia–reperfusion

ABSTRACT

S-Nitrosated human serum albumin (SNO-HSA) is a large molecular weight nitric oxide carrier in human plasma, and because of its many beneficial effects in different tests, it is currently under investigation as a cytoprotective agent. However, making SNO-HSA preparations is a complicated and time-consuming process. We found that binding of caprylic acid (CA) and N-acetyl-L-tryptophan (N-AcTrp) to defatted mercaptalbumin increased *S*-nitrosation by *S*-nitrosoglutathione (GS-NO) by making Cys-34 of HSA more accessible and by protecting it against oxidation, respectively. Fortunately, HSA solutions for clinical use contain high concentrations of CA and N-AcTrp as stabilizers. By making use of that fact it was possible to work-out a fast and simple procedure for producing SNO-HSA: incubation of a commercial HSA formulation with GS-NO for only 1 min results in *S*-nitrosation of HSA. The biological usefulness of such a preparation was tested in a rat ischemia–reperfusion liver injury model. Although our procedure for making SNO-HSA is fast and straightforward, the cytoprotective effect of the preparation was similar to, or better than, that of a preparation made in a more traditional way. The clinical development of SNO-HSA as a strong cytoprotective agent is under way using this method in collaboration with clinicians and industrial developers.

© 2010 Elsevier Inc. All rights reserved.

Introduction

Post-translational modifications are essential in their functional regulation. Among these, changes of the redox state of cysteine residues are of great importance. The sulfhydryl moiety can interact with nitric oxide (NO) and thereby form *S*-nitrosothiols [1–3]. *S*-Nitrosothiols may function as NO reservoirs and preserve the antioxidant and other activities of NO [4,5]. For example, it has been reported that *S*-nitrosated human serum albumin (SNO-HSA) may serve *in vivo* as a circulating reservoir for NO produced by the endothelial cells [6]. The reservoir function was also reported to be operative when application of SNO-HSA to animals suffering from ischemia–reperfusion injury minimized the extent of tissue damage associated with reperfusion [7–9]. Therefore, SNO-HSA is under investigation as a therapeutic agent in humans. However, efficient SNO-HSA preparations are difficult to produce.

HSA is a single, non-glycosylated polypeptide that organizes to form a heart-shaped protein with approximately 67% α-helix but no β-sheet [10]. Except for Cys-34, all of the 35 cysteine residues are involved in the formation of stabilizing disulfide bonds. Cys-34 represents the largest fraction of free thiols in the circulation (mercaptalbumin). The residue is located in "a crevice" on the surface in the N-terminal part of the protein, and such a location can impede the access of *S*-nitrosating agents to the sulfhydryl group. In addition, normally about half of the Cys-34 residues are oxidized or involved in ligand binding (non-mercaptalbumin), and that kind of hindrance could also make an efficient *S*-nitrosation difficult.

In previous investigations we found that binding of N-acetyl-L-tryptophanate (N-AcTrp) protects the sulfhydryl group of HSA against oxidation [11], and that binding of oleic acid increases *S*-nitrosation of HSA [12]. In the present work we found that

Abbreviations: HSA, human serum albumin; SNO-HSA, *S*-nitrosated HSA; GS-NO, *S*-nitrosoglutathione; N-AcTrp, N-acetyl-L-tryptophanate; CA, caprylic acid; ALT, alanine aminotransferase; AST, aspartate aminotransferase; HO-1, heme oxygenase-1.

* Corresponding author at: Department of Biopharmaceutics, Graduate School of Pharmaceutical Sciences, Kumamoto University, 5-1 Oe-honmachi, Kumamoto 862-0973, Japan. Fax: +81 96 362 7690.
E-mail address: otagirim@gpo.kumamoto-u.ac.jp (M. Otagiri).

[1] These two authors contributed equally to this work.

1089-8603/$ - see front matter © 2010 Elsevier Inc. All rights reserved.
doi:10.1016/j.niox.2010.05.002

simultaneous binding of N-AcTrp and caprylic acid (CA) greatly increased *S*-nitrosation of HSA by *S*-nitrosoglutathione (GS-NO) by protecting the sulfhydryl group against oxidation and by making it more accessible to GS-NO, respectively. HSA solutions for clinical use contain high concentrations of just N-AcTrp and CA, and we took advantage of that fact to work-out a simple, one-step method to make a biological active and stable SNO-HSA preparation which most probable also can be of clinical use, see the illustrative overview in Fig. 1.

Experimental procedures

Materials

HSA solutions (20%) were donated by the Chemo-Sera-Therapeutic Research Institute (Kumamoto, Japan). As stabilizers the formulation contained N-AcTrp (6.2 mol/mol HSA) and CA (5.3 mol/mol HSA). Part of the albumin was defatted by treatment with charcoal as described by Chen [13], dialyzed against deionized water, freeze-dried, and then stored at −20 °C until used. According to density analysis of Coomassie Brilliant Blue (CBB)-stained protein bands on 12.5% SDS–PAGE, the purity of albumin in the original solutions and of the defatted samples was more than 97%. N-AcTrp, CA and 1,4-dithiothreitol (DTT) were purchased from Sigma–Aldrich (St. Louis, MO). Sulfanilamide, naphthylethylenediamine-hydrochloride, $HgCl_2$, $NaNO_2$ and $NaNO_3$ were obtained from Nakalai Tesque (Kyoto, Japan). GS-NO, 5,5′-dithiobis-2-nitrobenzoic acid (DTNB) and diethylenetriaminepentaacetic acid (DTPA) were obtained from Dojindo Laboratories (Kumamoto, Japan). Other chemicals were of the best grades commercially available, and all solutions were made in deionized water. Sephadex G-25 desalting column (ϕ 1.6 × 2.5 cm) was from Amersham Pharmacia Biotech (Tokyo, Japan).

Preparation of HSA-ligand solutions

First, Cys-34 of defatted HSA was reduced by treatment with DTT as follows. HSA (300 μM) was incubated with DTT (molar ratio, protein:DTT = 1:10) for 5 min at 37 °C. After incubation, DTT was quickly removed by Sephadex G-25 gel filtration using 10 mM phosphate-buffered saline (pH 7.4) (PBS; Ca^{2+}, Mg^{2+} free). We checked that the final SH/HSA ratio was less than 1 by using the DTNB assay described below. Stock-solutions of 20 mM CA and 20 mM N-AcTrp were made in methanol–H_2O (1:1, v/v) and H_2O, respectively. Later, these stock-solutions were diluted with PBS. In all cases, the resulting solutions were mixed with PBS containing HSA. The final methanol concentrations in the CA-containing solutions were 0.75% or less. The protein content of all protein preparations used in this study was determined by the Bicinchoninic acid protein assay.

Accessibility of Cys-34 in the presence and absence of ligands

DTT-treated HSA (100 μM) was incubated with 0.5 mM Ellman's reagent, DTNB, for 60 min at room temperature. During incubation, the absorbance of the samples was monitored at 405 nm. The accessibility was evaluated as A_5/A_{60}, where A_5 and

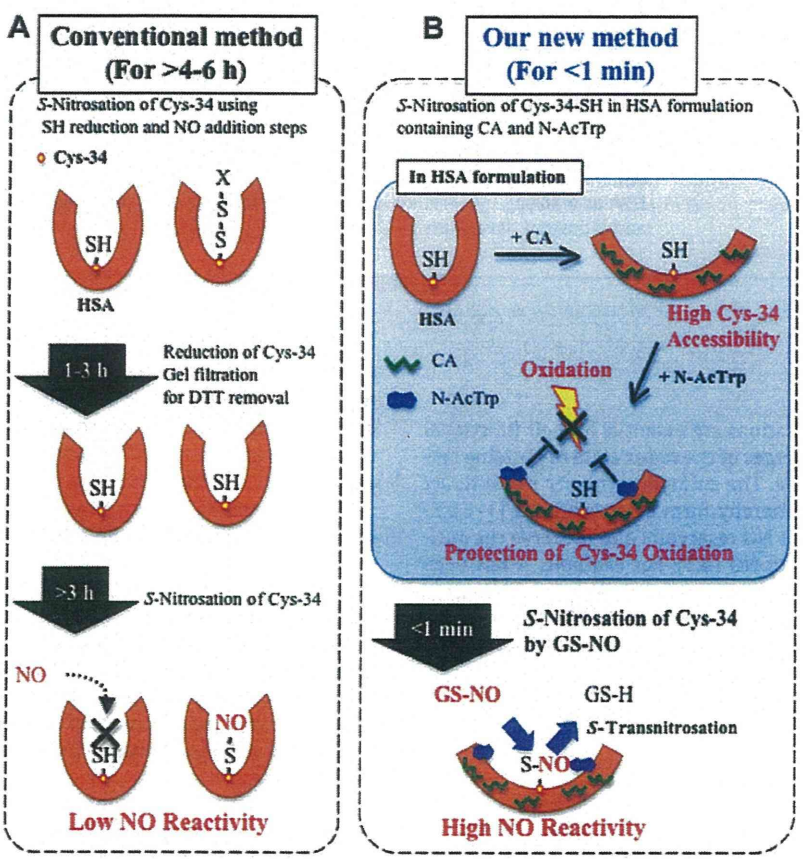

Fig. 1. Mechanism of a novel SNO-HSA preparation strategy using HSA formulation and GS-NO. The conventional method (A) contains two time-consuming steps (SH reduction and NO addition), which take more than 4–6 h to complete. On the other hand, our new method (B) contains only one step (GS-NO incubation), which takes less than 1 min. In case of our method, CA and N-AcTrp contained in HSA formulations play the roles of not only stabilizers but also as a Cys-34 accessible inducer and a Cys-34 oxidation inhibitor, respectively. The presence of these two ligands makes it possible to *S*-nitrosate HSA within 1 min.

A_{60} are the sample absorbance after 5 and 60 min (maximal absorbance), respectively, of incubation with DTNB [14].

SH content of Cys-34 in the presence and absence of ligands

The amount of free SH-groups was also estimated with Ellman's reagent, DTNB. Briefly, HSA (100 μM) was incubated with 0.5 mM DTNB for 60 min at room temperature, and afterwards the absorbance at 405 nm was measured. The thiol concentration was calculated from a standard curve prepared with cysteine.

Oxidation of Cys-34 and protein polymerization by heat treatment in the presence and absence of ligands

DTT-treated HSA (100 μM) without or with ligand (5 mol/mol HSA) was incubated in PBS (pH 7.4) for 15 or 60 min at 60 °C. The mercaptalbumin fraction was determined from a standard curve prepared with cysteine using the DTNB assay. Any changes in molecular weight and aggregation of heated HSA samples were visualized by non-reduced 10% SDS–PAGE with 3 μg of protein in each lane.

S-Nitrosation of HSA in the presence and absence of ligands

SNO-HSA was prepared with protection against light and according to previous reports [15,16]. Briefly, DTT-treated HSA (100 μM) without or with ligand (5 mol/mol HSA) or the original solution from Chemo-Sera-Therapeutic Research Institute was incubated with GS-NO as NO donor (molar ratio, protein:NO donor = 1:5) in PBS for 1, 15 or 60 min at 37 °C. To remove the NO donor, the *S*-nitrosated products were applied to a Sephadex G-25 column, eluted with PBS containing 0.5 mM DTPA, and concentrated by ultrafiltration. These samples were stored at −80 °C until analyzed. For the *in vivo* ischemia–reperfusion studies, the SNO-HSA samples with and without ligand were adjusted to the same *S*-nitrosation efficiency by means of different incubation times with GS-NO. Actually, the HSA samples with or without ligand were incubated with GS-NO for 1 or 60 min, respectively.

Determination of S-nitrosation efficiency

The amounts of the *S*-nitroso moiety of SNO-HSA were quantified by HPLC coupled with a flow-reactor system, as previously reported [15,17]. The HPLC column was a gel filtration column for *S*-nitrosated proteins (ϕ 8 × 300 mm), Diol-120, YMC, Kyoto, Japan. Briefly, the eluate from the HPLC column was mixed with a $HgCl_2$ solution to decompose SNO compounds to yield NO_2^- (via NO^+). The NO_2^- generated was then detected after reaction with Griess reagent in the flow-reactor system.

CD spectroscopy

CD spectra were measured at 25 °C using a J-720-type spectropolarimeter (JASCO, Tokyo, Japan). Far-UV and near-UV spectra were recorded at protein concentrations of 5 and 15 μM, respectively, in 20 mM sodium phosphate buffer (pH 7.4). For calculation of mean residue ellipticity, [θ], the molecular weight of the albumins was taken as 66,500.

Cytoprotective effect of SNO-HSA in vivo

A rat ischemia–reperfusion liver injury model served for investigation of the cytoprotective effect of SNO-HSA, according to a previous report [16]. Male Wistar rats weighing between 200 and 230 g (Kyudo, Inc., Kumamoto, Japan) were used. The animals were fasted for 9 h before surgery but were allowed access to water. The rats were anesthetized with ether during the operation. After the abdomen was shaved and disinfected with 70% ethanol, a complete midline incision was made. The portal vein and hepatic artery were exposed and cross-clamped for 30 min with a noncrushing microvascular clip. Saline, as the vehicle control, GS-NO or DTT-treated HSA without or with *S*-nitrosation or the original formulation without or with *S*-nitrosation (0.1 μmol protein (0.03 μmol SNO)/rat) were given via the portal vein immediately after reperfusion was initiated. Then the abdomen was closed in two layers with 2–0 silk. The rats were kept under warming lamps until they awakened and became active. Because blood loss caused by frequent blood sampling could affect liver functions, the animals were sacrificed by taking whole circulating blood via abdominal aorta under anesthesia at various time points after reperfusion was initiated. Plasma alanine aminotransferase (ALT) and aspartate aminotransferase (AST) activities were measured by using a sequential multiple AutoAnalyzer system from Wako Chemicals, with activities expressed in international units per liter. All animal experiments were carried out according to the guidelines of the Laboratory Protocol of Animal Handling, Graduate School of Medical Sciences, Kumamoto University.

Purification of intracellular proteins and Western blot analysis

Frozen liver samples, originally taken 6 h after hepatic ischemia–reperfusion, were homogenized in a lysis buffer (50 mM HEPES, 5 mM EDTA, and 50 mM NaCl; pH 7.5) containing protease inhibitors (10 mg/mL aprotinin, 1 mM PMSF, and 10 mg/mL leupeptin). Supernatant was taken after centrifugation at 15,000g. Equal amounts of protein from the supernatant were loaded onto 12.5% SDS–PAGE gels and blotted onto polyvinylidine difluoride membranes (Millipore). Polyclonal antibody against rat heme oxygenase-1 (HO-1; StressGen) and horseradish conjugated secondary antibody (Jackson ImmunoResearch) were used at 1:2000 and 1:5000 dilutions, respectively. The ECL Western blotting system (Amersham Life Sciences) was used for detection. Bands were visualized and quantified using a lumino-analyzer (LAS-1000, Fuji photo Film). Density of the bands for HO-1 and β-actin was quantitatively analyzed using the NIH Image J Software.

Statistical analysis

The statistical significance of collected data was evaluated using the ANOVA analysis followed by Newman–Keuls method for more than 2 means. Differences between groups were evaluated by the Student's *t* test. $P < 0.05$ was regarded as statistically significant.

Results

Effect of ligand binding on the SH-accessibility of Cys-34

The effect of CA and/or N-AcTrp binding on the SH-accessibility of defatted, DTT-treated HSA was evaluated by the DTNB assay. Binding of 1–5 mol CA/mol HSA increased significantly and in a dose-dependent manner the accessibility of the SH-group (Fig. 2A). By contrast, addition of 5 mol of N-AcTrp per mol of HSA had no significant effect on SH-accessibility (Fig. 2B). Furthermore, addition of N-AcTrp had no influence on the improving effect of CA (Fig. 2B).

Protective effect of ligands on oxidation and aggregation of mercaptalbumin exposed to heat treatment

Defatted, DTT-treated HSA without and with ligands (N-AcTrp and/or CA) was incubated at 60 °C. Heat incubation was used, be-

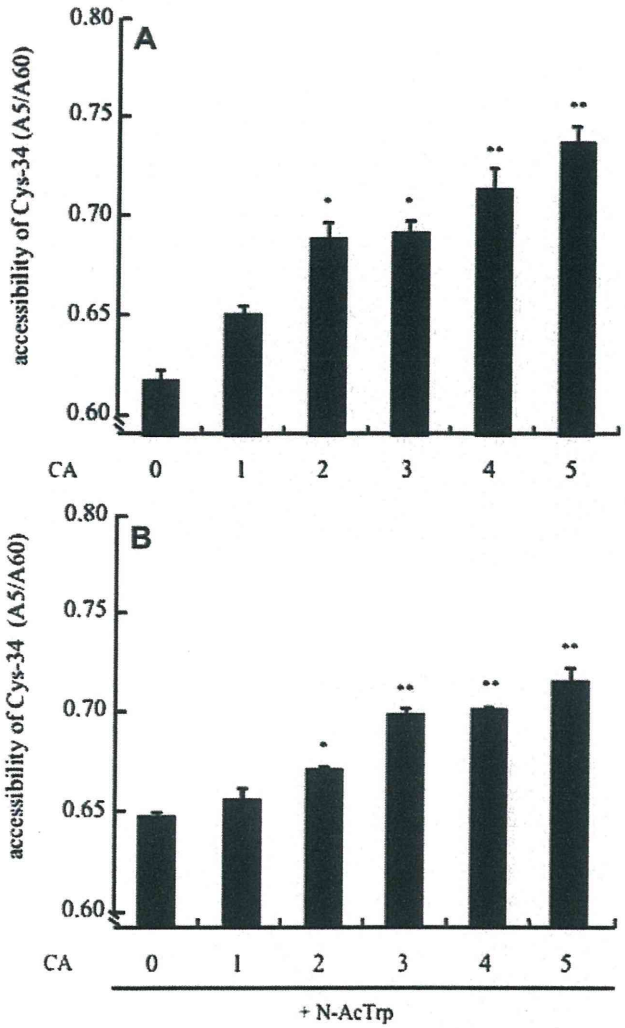

Fig. 2. Effect of ligand binding on the SH-accessibility of Cys-34. The effect of CA (CA/HSA = 0, 1, 2, 3, 4, 5) on the SH-accessibility of defatted, DTT-treated HSA was studied in the absence (A) and presence of N-AcTrp (N-AcTrp/HSA = 5) (B). DTT-treated HSA (100 μM) was incubated with 0.5 mM Ellman's reagent, DTNB, for 60 min at room temperature. The accessibility was evaluated as the ratio of DTNB absorbance at 405 nm after 5 and 60 min of incubation (A_5/A_{60}). A_5 and A_{60} are the sample absorbance at 405 nm after 5 min (initial rate period) and 60 min (maximal absorbancy), respectively, of incubation with DTNB. Data are expressed as means ± SEM ($n = 4$). *, $p < 0.05$, **, $p < 0.01$, compared with control (CA = 0).

cause in this way we could study both thiol oxidation and protein aggregation [11,18,19]. From Table 1 it is seen that N-AcTrp is an effective protector of the sulfhydryl group against heat-facilitated oxidation; less than 10% of the groups have been oxidized after 60 min of incubation. By contrast, binding of CA increases oxidation; after 60 min of heat treatment ca. 75% of Cys-34 have been oxidized, whereas only ca. 35% of the groups have been modified in the absence of ligands. Finally, simultaneous binding of CA diminishes somewhat the protective effect of N-AcTrp. The increasing effect of CA on oxidation is most probably due to the fact that CA binding increases the accessibility of Cys-34 (see above). Often oxidation of cysteine residues is accompanied by protein aggregation. Whether or not this has taken place in our heat-treated HSA samples was analyzed for by using non-reduced SDS–PAGE (Fig. 3). Lane 1 shows no clear presence of light or heavy aggregated HSA in the non-heated sample. Heating for 15 min at 60 °C actually results in formation of both types of aggregations (lane 2), and heating for 60 min results in a major fraction of heavy aggregation (lane 6). Addition of N-AcTrp diminishes aggregation (lanes 3 and 7); especially the formation of heavy aggregation is strongly depressed. By contrast, binding of CA has no inhibitory effect on aggregation (lanes 4 and 8). Interestingly, apparently CA has no influence on the protective effect of N-AcTrp (lanes 5 and 9). Thus, N-AcTrp, but not CA, minimizes HSA aggregation and protects Cys-34 against oxidation.

Table 1
Mercaptalbumin ratio (% of total albumin) after oxidation by heat incubation.

Heal incubation time (mm)	0	15	60
HSA alone	82.0 ± 2.4	75.6 ± 3.1	54.3 ± 3.9
HSA with N-AcTrp	82.0 ± 2.4	77.5 ± 2.6	74.6 ± 2.6**
HSA with CA	82.0 ± 2.4	21.3 ± 5.9*	19.4 ± 8.4**
HSA with CA and N-AcTrp	82.0 ± 2.4	63.9 ± 4.0*	61.0 ± 5.0*

Results are given as means ± SEM ($n = 6$).
* $P < 0.05$ as compared with HSA alone.
** $P < 0.01$ as compared with HSA alone.

Improving effects of ligand binding on S-nitrosation of HSA

Now, we investigated whether an increased accessibility to Cys-34 (caused by CA binding) and/or protection of the residue against oxidation and aggregation (caused by N-AcTrp binding) can promote *S*-nitrosation of HSA. Incubation of defatted, DTT-treated HSA alone with GS-NO for 60 min resulted in the formation of 0.31 mol *S*-nitroso moieties per mol of HSA (Table 2). This value, and those determined at 1 and 15 min of incubation, is not changed by addition of N-AcTrp. By contrast, at all incubation times CA significantly increased *S*-nitrosation. Simultaneous addition of both ligands increased this effect further, and after 1 min of incubation the number of *S*-nitroso moieties (0.42 mol SNO/mol HSA) is even higher than that obtained after 60 min of HSA without ligand. Thus, co-binding of CA and N-AcTrp results in efficient and fast *S*-nitrosation of HSA. HSA formulations for clinical applications usually contain high concentrations of CA and N-AcTrp for stabilizing and protecting the protein against oxidation during the heat treatment performed for destroying potential contamination with

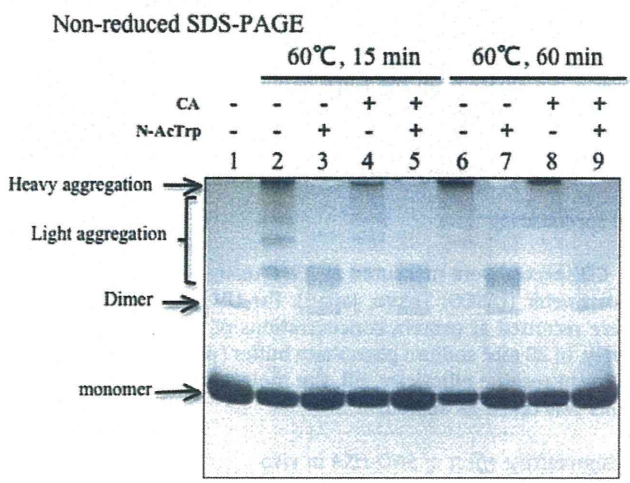

Fig. 3. Effect of ligands on aggregation of heat-treated mercaptalbumin. Defatted, DTT-treated HSA without or with ligand (5 mol/mol HSA) was incubated in PBS (pH 7.4) for 15 or 60 min at 60 °C. Afterwards, protein samples (3 μg) were analyzed by non-reduced 10% SDS–PAGE; the gel was stained by CBB. Lane 1 represents non-heated HSA. The arrows indicate heavy aggregation, light aggregation, dimer and monomer from the top.

Table 2
S-Nitroso moieties (SNO mol/mol USA) after incubation with GS-NO.

GS-NO incubation time (min)	0	1	15	60
HSA alone	0.00 ± 0.00	0.06 ± 0.03	0.12 ± 0.03	0.31 ± 0.03
HSA with N-AcTrp	0.00 ± 0.00	0.08 ± 0.02	0.13 ± 0.02	0.33 ± 0.06
HSA with CA	0.00 ± 0.00	0.29 ± 0.06**	0.31 ± 0.06**	0.41 ± 0.08**
HSA with CA and N-AcTrp	0.00 ± 0.00	0.42 ± 0.09**	0.45 ± 0.10**	0.51 ± 0.09**
HSA formulation	0.00 ± 0.00	0.35 ± 0.05**	0.41 ± 0.10**	0.45 ± 0.09**

Results are given as means ± SEM (n = 3–10).
** $P < 0.01$, as compared with HSA alone.

viral or other biological agents [11]. We used the solutions from Chemo-Sera-Therapeutic Research Institute as an illustrative example, and this formulation has 5–6 mol of each of the two ligands per mol of HSA. Furthermore, it has a high percentage of mercaptalbumin, i.e. 71 ± 8% (n = 6). Therefore, we investigated whether a simple incubation of the formulation with GS-NO would result in significant amounts of SNO-HSA. As seen from Table 2, this one-step procedure also resulted in an efficient and fast *S*-nitrosation of HSA.

Physicochemical properties and stability of S-nitrosated HSA

According to reduced and non-reduced SDS–PAGE, the one-step *S*-nitrosation of formulation HSA did not result in the formation of dimer via disulfide bond formation, fragmentation or other gross conformational changes (Fig. 4A). Any minor conformational changes were examined for by using circular dichroism spectroscopy. The far-UV spectra (Fig. 4B) and the near-UV spectra (Fig. 4C) show that *S*-nitrosation of Cys-34 had no evident effect on the secondary or tertiary structure of HSA. Previous examinations with non-reducing SDS–PAGE revealed that *S*-nitrosation of defatted, DTT-treated HSA only results in, if any, changes in the tertiary structure of the protein [9]. Thus, our data propose that *S*-nitrosation does not induce significant conformational changes in any of our protein preparations. The stability of SNO-HSA with 5 mol of CA and N-AcTrp per mol of protein was tested in two different ways. First, the half-life of the *S*-nitroso moiety of SNO-HSA with the ligands was 50 days in phosphate buffer, pH 7.4, in the dark. Without the ligands the half-life was only 25 days. Second, lyophilization with CA and N-AcTrp resulted in only a slight decrease (10%) in *S*-nitroso content. Thus, SNO-HSA with CA and N-AcTrp is very stable.

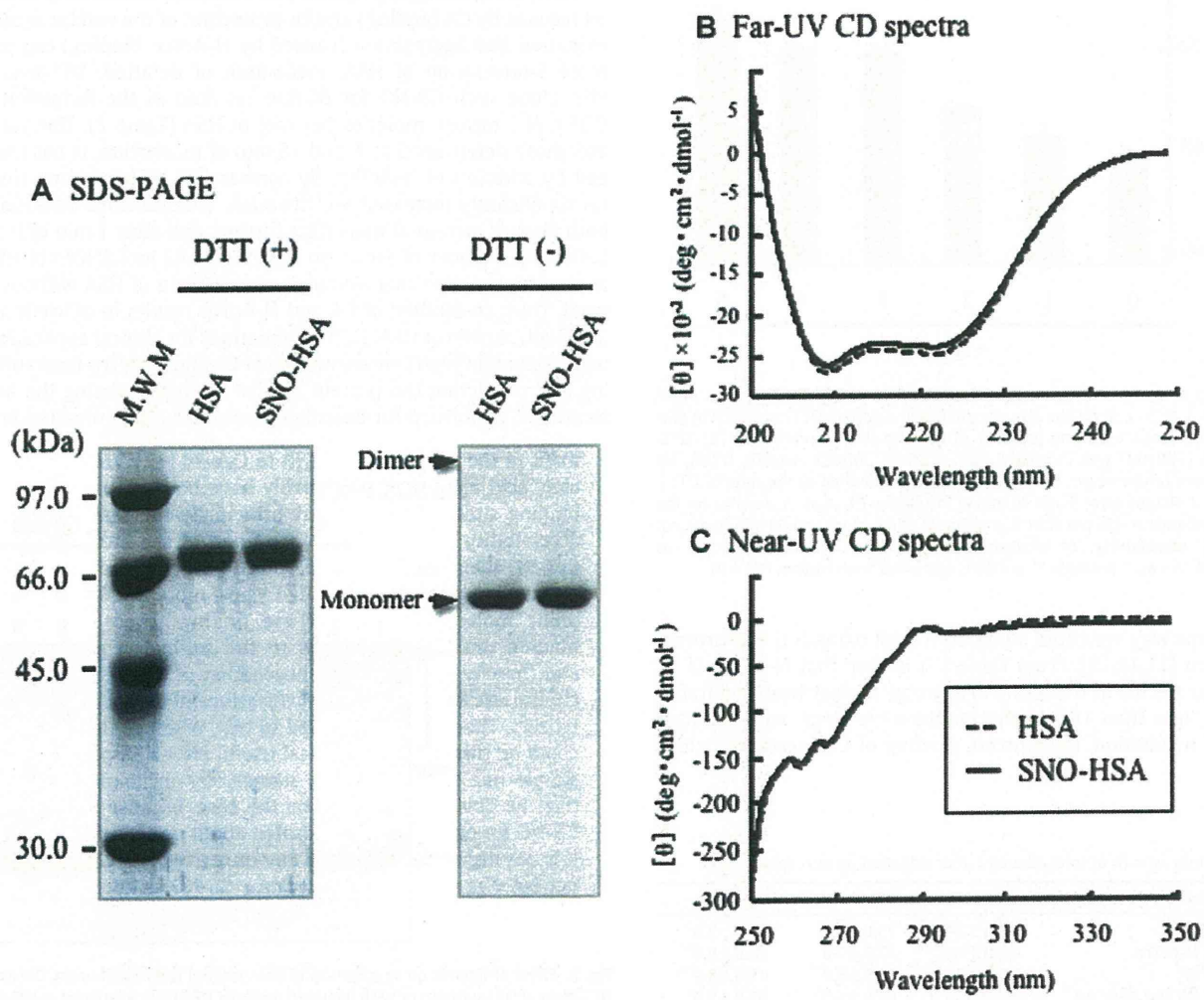

Fig. 4. Structural integrity of HSA and SNO-HSA. (A) Reduced and non-reduced SDS–PAGE of HSA and SNO-HSA. 1 μg of protein was added to each lane, and the gel was stained by CBB. Molecular mass markers are indicated at the left of the gel. B and C show far-UV and near-UV CD spectra, respectively, of HSA and SNO-HSA. The proteins were unmodified and *S*-nitrosated HSA formulation.

Cytoprotective effect of SNO-HSA against ischemia–reperfusion injury

We tested the biological usefulness of the one-step SNO-HSA preparation by studying its cytoprotective effect in an ischemia–reperfusion liver injury model in rats [9,16,20]. Previous studies with SNO-HSA showed that a quantity of 0.1 μmol protein/rat was most suitable for this kind of experiment [9]. Therefore, we used the same quantity of SNO-HSA in this study. To evaluate liver injury, we measured the extracellular release of the liver enzymes ALT and AST via plasma enzyme values. Without adding albumin, the ALT-values increased to a maximum at 1 h after reperfusion. After 2 h the value was slightly lower and then decreased further and gradually during 24 h. Principally the same results were obtained for AST (data not shown). Administration of DTT-treated HSA, of the original HSA formulation or of GS-NO at the beginning of reperfusion did not modify liver damage (Fig. 5A). However, a significant reduction in the release of ALT was observed in rats treated with SNO-HSA, which had been made by incubating defatted, DTT-treated HSA (5 mol CA and N-AcTrp/mol HSA) with GS-NO for 60 min. The same, or even better, cytoprotection was obtained after injecting SNO-HSA, which had been made by incubating the original HSA formulation with GS-NO for only 1 min. Again, principally the same results were obtained for AST (data not shown). We have also determined the expression of the intracellular, cytoprotective enzyme HO-1 in the liver cells 6 h after reperfusion. Fig. 5B shows that if DTT-treated HSA, HSA formulation or GS-NO was injected at the beginning of reperfusion, a pronounced induction of HO-1 took place. However, the most pronounced induction took place after injection of SNO-HSA. As an internal control we determined the amount of β-actin (Fig. 5B). The density of the HO-1 and β-actin bands were quantified and related to each other. Also this type of analysis showed that administration of SNO-HSA resulted in a very pronounced induction of HO-1. The HO-1 expression increased as follows: DTT-treated HSA = HSA formulation < GS-NO < SNO-HSA, which had been made by incubating DTT-treated HSA (5 mol CA and N-AcTrp/mol HSA) with GS-NO for 60 min < SNO-HSA, which had been made by incubating the original HSA formulation with GS-NO for only 1 min. Thus, in addition to *S*-nitrosation, binding of CA and N-AcTrp improved the cytoprotective effect. *S*-Nitrosothiols such as SNO-HSA can exert cytoprotective effects in different ways. In addition to inducing HO-1, the effect can be brought about by, for example, maintenance of tissue blood flow, suppression of neutrophil infiltration and reduction of apoptosis in the liver [16].

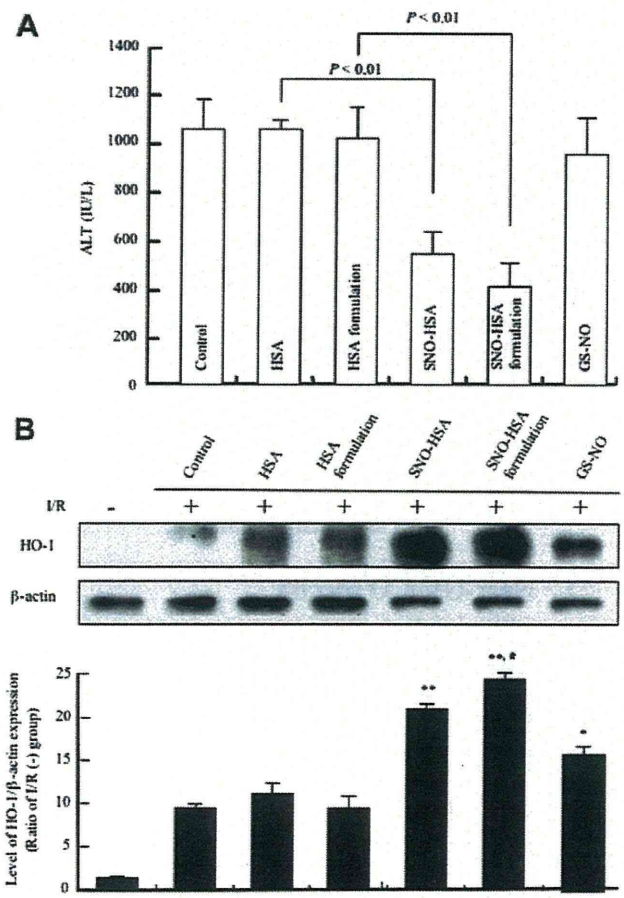

Fig. 5. Serum levels of ALT and Western blot of HO-1 and β-actin in liver cells after hepatic ischemia–reperfusion in rats. (A) Saline (control), HSA, HSA formulation, SNO-HSA, SNO-HSA formulation or GS-NO (the same amount of SNO administration as with SNO-HSA) was injected at the beginning of reperfusion (0 min), and the activities of ALT were measured at 60 min after reperfusion. (B) Western blot of HO-1 and β-actin in liver cells 6 h after hepatic ischemia–reperfusion. I/R (−) are results from rats, which had not been subject to ischemia–reperfusion. The density of the bands for HO-1 and β-actin was quantitatively analyzed using the NIH Image J Software. Data are expressed as means ± SEM ($n = 4$). *, $p < 0.05$, **, $p < 0.01$, compared with I/R (−). #, $p < 0.05$, compared with SNO-HSA.

Discussion

SNO-HSA has been shown to be cytoprotective against free radical mediated damage and microvascular injury associated with ischemia–reperfusion or hemorrhagic shock as well as acute lung injury in a murine model of sickle cell disease. Therefore, SNO-HSA is under investigation as a therapeutic agent in humans. However, existing methods for making SNO-HSA preparations are complicated and time-consuming, see the illustrative overview in Fig. 1. In the first parts of this work, we observed that binding of CA and N-AcTrp resulted in a very pronounced increment in *S*-nitrosation of HSA when incubated with GS-NO. The increment is most probably caused by an easier access of GS-NO to the sulfhydryl group of Cys-34 and protection of the residue against oxidation. In addition, the presence of the ligands resulted in an increased stability of the *S*-nitrosated product. We have previously found that binding of oleic acid resulted in an almost linear increment in the reactivity of DTNB to Cys-34 [12]. Thus, even though oleic acid and CA most probably have both common and private binding sites [21], they exert principally the same effect on the accessibility of Cys-34. Because none of the fatty acids bind to Cys-34, their effects must be due to binding-induced conformational changes of HSA making Cys-34 more accessible to electrophilic molecules [12,14]. These findings show that fatty acid binding can ease the access to the sulfhydryl group of Cys-34 and thereby improve the *S*-nitrosation of HSA. HSA solutions for clinical use contain high concentrations of CA and N-AcTrp as stabilizers. Therefore, we decided to test, whether such formulations could be turned into biological useful SNO-HSA preparations by a simple one-step procedure, namely by incubation with GS-NO (Fig. 1). This was found to be the case, because incubation with GS-NO for only 1 min *S*-nitrosated about one third of the albumin. It is not necessary to remove any unreacted GS-NO from the product by, e.g., gel filtration, because GS-NO is eliminated fast and apparently without secondary effects from the circulation [9]. We tested the biological usefulness of the preparation by studying its cytoprotective effect in an ischemia–reperfusion liver injury model. The results showed that it had a superior biological activity, and that CA and N-AcTrp binding improved the effect. The present findings can probably be of practical use, because instead of giving patients a simple HSA formulation, the formulation can easily and

fast be upgraded to a solution with a high concentration of SNO-HSA, which could be of greater help to the patient and have a broader application. The clinical development of SNO-HSA as a strong cytoprotecting agent is under way using our simple method in collaboration with clinicians of hospital and developers of drug industry.

Acknowledgments

This work was supported in part by Grants-in-Aid from the Japan Society for the Promotion of Science (JSPS), a Grant-in-Aid from the Ministry of Education, Culture, Sports, Science and Technology, Japan (18390051), and by Fonden af 1870. Thanks are also due to members of the Gene Technology Center in Kumamoto University for their important contributions to the experiments.

References

[1] L.J. Ignarro, P.J. Kadowitz, W.H. Baricos, Evidence that regulation of hepatic guanylate cyclase activity involves interactions between catalytic site –SH groups and both substrate and activator, Arch. Biochem. Biophys. 208 (1981) 75–86.
[2] L.J. Ignarro, H. Lippton, J.C. Edwards, W.H. Baricos, A.L. Hyman, P.J. Kadowitz, C.A. Gruetter, Mechanism of vascular smooth muscle relaxation by organic nitrates, nitrites, nitroprusside and nitric oxide: evidence for the involvement of S-nitrosothiols as active intermediates, J. Pharmacol. Exp. Ther. 218 (1981) 739–749.
[3] L.J. Ignarro, B.K. Barry, D.Y. Gruetter, J.C. Edwards, E.H. Ohlstein, C.A. Gruetter, W.H. Baricos, Guanylate cyclase activation of nitroprusside and nitrosoguanidine is related to formation of S-nitrosothiol intermediates, Biochem. Biophys. Res. Commun. 94 (1980) 93–100.
[4] N. Hogg, Biological chemistry and clinical potential of S-nitrosothiols, Free Rad. Biol. Med. 28 (2000) 1478–1486.
[5] M.W. Foster, T.J. McMahon, J.S. Stamler, S-nitrosation in health and disease, Trends Mol. Med. 9 (2003) 160–168.
[6] J.S. Stamler, D.I. Simon, J.A. Osborne, M.E. Mullins, O. Jaraki, T. Michel, D.J. Singel, J. Loscalzo, S-nitrosation of proteins with nitric oxide: synthesis and characterization of biologically active compounds, Proc. Natl. Acad. Sci. USA 89 (1992) 444–448.
[7] S. Hallstrom, H. Gasser, C. Neumayer, A. Fugl, J. Nanobashvili, A. Jakubowski, I. Huk, G. Schlag, T. Malinski, S-nitroso human serum albumin treatment reduces ischemia/reperfusion injury in skeletal muscle via nitric oxide release, Circulation 105 (2002) 3032–3038.
[8] M. Dworschak, M. Franz, S. Hallstrom, S. Semsroth, H. Gasser, M. Haisjackl, B.K. Podesser, T. Malinski, S-nitroso human serum albumin improves oxygen metabolism during reperfusion after severe myocardial ischemia, Pharmacology 72 (2004) 106–112.
[9] Y. Ishima, T. Sawa, U. Kragh-Hansen, Y. Miyamoto, S. Matsushita, T. Akaike, M. Otagiri, S-nitrosylation of human variant albumin Liprizzi (R410C) confers potent antibacterial and cytoprotective properties, J. Pharmacol. Exp. Ther. 320 (2007) 969–977.
[10] T. Peters Jr., All About Albumin: Biochemistry, Genetics, and Medical Applications, Academic Press, San Diego, 1996.
[11] M. Anraku, Y. Tsurusaki, H. Watanabe, T. Maruyama, U. Kragh-Hansen, M. Otagiri, Stabilizing mechanisms in commercial albumin preparations: octanoate and N-acetyl-L-tryptophanate protect human serum albumin against heat and oxidative stress, Biochim. Biophys. Acta 1702 (2004) 9–17.
[12] Y. Ishima, T. Akaike, U. Kragh-Hansen, S. Hiroyama, T. Sawa, T. Maruyama, T. Kai, M. Otagiri, Effects of endogenous ligands on the biological role of human serum albumin in S-nitrosylation, Biochem. Biophys. Res. Commun. 364 (2007) 790–795.
[13] R.F. Chen, Removal of fatty acids from serum albumin by charcoal treatment, J. Biol. Chem. 242 (1967) 173–181.
[14] Y.A. Gryzunov, A. Arroyo, J.L. Vigne, Q. Zhao, V.A. Tyurin, C.A. Hubel, R.E. Gandley, Y.A. Vladimirov, R.N. Taylor, V.E. Kagan, Binding of fatty acids facilitates oxidation of cysteine-34 and converts copper-albumin complexes from antioxidants to prooxidants, Arch. Biochem. Biophys. 413 (2003) 53–66.
[15] T. Akaike, K. Inoue, T. Okamoto, H. Nishino, M. Otagiri, S. Fujii, H. Maeda, Nanomolar quantification and identification of various nitrosothiols by high performance liquid chromatography coupled with flow reactors of metals and Griess reagent, J. Biochem. (Tokyo) 122 (1997) 459–466.
[16] N. Ikebe, T. Akaike, Y. Miyamoto, K. Hayashida, J. Yoshitake, M. Ogawa, H. Maeda, Protective effect of S-nitrosylated alpha(1)-protease inhibitor on hepatic ischemia–reperfusion injury, J. Pharmacol. Exp. Ther. 295 (2000) 904–911.
[17] K. Inoue, T. Akaike, Y. Miyamoto, T. Okamoto, T. Sawa, M. Otagiri, S. Suzuki, T. Yoshimura, H. Maeda, Nitrosothiol formation catalyzed by ceruloplasmin. Implication for cytoprotective mechanism in vivo, J. Biol. Chem. 274 (1999) 27069–27075.
[18] M. Anraku, Y. Kouno, T. Kai, Y. Tsurusaki, K. Yamasaki, M. Otagiri, The role of N-acetyl-methioninate as a new stabilizer for albumin products, Int. J. Pharm. 329 (2007) 19–24.
[19] N.K. Holm, S.K. Jespersen, L.V. Thomassen, T.Y. Wolff, P. Sehgal, L.A. Thomsen, G. Christiansen, C.B. Andersen, A.D. Knudsen, D.E. Otzen, Aggregation and fibrillation of bovine serum albumin, Biochim. Biophys. Acta 1774 (2007) 1128–1138.
[20] Y. Ishima, T. Akaike, U. Kragh-Hansen, S. Hiroyama, T. Sawa, A. Suenaga, T. Maruyama, T. Kai, M. Otagiri, S-nitrosylated human serum albumin-mediated cytoprotective activity is enhanced by fatty acid binding, J. Biol. Chem. 283 (2008) 34966–34975.
[21] U. Kragh-Hansen, H. Watanabe, K. Nakajou, Y. Iwao, M. Otagiri, Chain length-dependent binding of fatty acid anions to human serum albumin studied by site-directed mutagenesis, J. Mol. Biol. 363 (2006) 702–712.

Journal of Controlled Release 145 (2010) 9–16

Contents lists available at ScienceDirect

Journal of Controlled Release

journal homepage: www.elsevier.com/locate/jconrel

Genetically engineered mannosylated-human serum albumin as a versatile carrier for liver-selective therapeutics

Kenshiro Hirata [a,1], Toru Maruyama [a,b,1], Hiroshi Watanabe [b], Hitoshi Maeda [a], Keisuke Nakajou [c], Yasunori Iwao [a], Yu Ishima [a], Hidemasa Katsumi [d,e], Mitsuru Hashida [d], Masaki Otagiri [a,f,*]

[a] Department of Biopharmaceutics, Graduate School of Pharmaceutical Sciences, Kumamoto University, 5-1 Oe-honmachi, Kumamoto 862-0973, Japan
[b] Center for Clinical Pharmaceutical Sciences, Kumamoto University, 5-1 Oe-honmachi, Kumamoto 862-0973, Japan
[c] The Pharmaceutical Research Center, Nipro Corporation 3023 Nojicho, Kusatsu, Shiga 525-0055, Japan
[d] Department of Drug Delivery Research, Graduate School of Pharmaceutical Sciences, Kyoto University, Sakyo-ku, Kyoto 606-8501, Japan
[e] Department of Biopharmaceutics, Kyoto Pharmaceutical University, Yamashina-ku, Kyoto 607-8414, Japan
[f] Faculty of Pharmaceutical Sciences, Sojo University, 4-22-1 Ikeda, Kumamoto 860-0822, Japan

ARTICLE INFO

Article history:
Received 23 October 2009
Accepted 13 March 2010
Available online 19 March 2010

Keywords:
Human serum albumin
Recombinant albumin
Mannosylation
Nitric oxide
Ischemia reperfusion

ABSTRACT

Human serum albumin (HSA), a non-glycosylated protein, is widely employed as carrier for drug delivery systems. A series of recombinant, mannosylated-HSA mutants (Man-rHSAs: D63N, A320T and D494N) and their triple mutant (TM-rHSA: D63N/A320T/D494N) were prepared, that can be selectively delivered to the liver *via* mannose receptor (MR) on the liver non-parenchymal cells. A pharmacokinetic analysis of ^{111}In-Man-rHSAs in mice showed that they were rapidly cleared from the blood circulation, and were largely taken up by the liver rapidly in the order: TM-rHSA > D494N ≫ A320T = D63N, consistent with their degree of mannosylation. *In vivo* competition experiments with an excess amount of chemically modified Man-BSA or mannan suggested that the hepatic uptake of TM-rHSA was selectively mediated by MR on Kupffer cells. Lastly, a TM-rHSA–NO conjugate, *S*-nitrosylated TM-rHSA, effectively delivered NO to the liver and then exhibited a significant inhibitory effect against hepatic ischemia/reperfusion injury model rats, accompanied by the induction of heme oxygenase-1.
Crown Copyright © 2010 Published by Elsevier B.V. All rights reserved.

1. Introduction

Human serum albumin (HSA) is the most abundant protein in plasma. The molecule is comprised of 585 amino acid residues with a MW of 66.7 kDa. HSA possesses multiple functions, including the maintenance of colloid osmotic pressure in plasma and the transport of various endogeneous substances and metabolite [1]. Because HSA has a simple molecular structure and is highly stable, it is frequently used to reduce immunogenicity associated with other therapeutics [1]. Thus, HSA is widely employed as a versatile carrier in drug delivery systems to improve pharmacokinetics and stability etc., thus improving the efficacy of therapeutics.

Since HSA does not contain canonical acceptor sequences (Asn-X-Thr/Ser tripeptide) required for *N*-glycosylation in its primary structure, it is not glycosylated in its native state. More than 60 genetic variants of HSA have been reported to date [2]. Researchers in several laboratories (including ours) have characterized the molecular, structural, biochemical and pharmacokinetic properties and stability of these genetic variants. Among them, three glycosylated HSA variants (albumin Darakallia, D63N; albumin Redhill, A320T; and albumin Casebrook, D494N) have been identified [3–5] because these mutant molecules contain the consensus sequence required for *N*-glycosylation. These variants behaved like wild-type HSA and possess similar properties. This leads to the conclusion that they might be potentially useful in therapeutic applications, especially as a carrier for a drug delivery system.

A number of suitable strategies for liver-selective targeting systems have been developed that involve the use of albumins that are chemically modified with substrates or ligands, such as sugars and peptides that bind receptors on the liver surface. One particularly interesting strategy involves the sugar recognition mechanism in which receptors recognize the corresponding sugars on the non-reducing terminal of sugar chains that are attached to albumin thereby mediating cellular uptake. Among these, chemically mannosylated (Man)-albumins have receive considerable attention because mannose receptors (MR), which specifically recognize ligands containing a terminal non-reducing D-mannose, N-acetylgluocosamine, or L-fucose, are expressed mainly on liver non-parenchymal cells, including Kupffer cells and sinusoidal endothelial cell [6,7]. Previous

Abbreviations: BSA, bovine serum albumin; CBB, Coomassie brilliant blue; DTPA, diethylenetriaminepentaacetic acid; DTT, dithiothreitol; Gal-BSA, galactosylated-BSA; GlcNAc, N-acetyl glucosamine; GSNO, *S*-nitroso glutathione; HO-1, heme oxygenase-1; HSA, human serum albumin; IR, ischemia reperfusion; man, mannose; man-BSA, mannosylated-BSA; Man-rHSAs, mannosylated-recombinant HSA mutants; PAS-stain, periodic acid Schiff-stain; ROS, reactive oxygen species; *S*NO-HSA, *S*-nitrosylated HSA; TM, triple mutant.

* Corresponding author. Tel.: +81 96 371 4150; fax: +81 96 362 7690.
E-mail address: otagiri@gpo.kumamoto-u.ac.jp (M. Otagiri).
[1] These authors contributed equally to this study.

0168-3659/$ – see front matter. Crown Copyright © 2010 Published by Elsevier B.V. All rights reserved.
doi:10.1016/j.jconrel.2010.03.010

studies have clearly demonstrated that chemically modified Man-albumins are largely taken up by the liver *via* an MR-mediated mechanism. Despite such selective delivery, chemically modified Man-HSA has several limitations, for instance, its heterogeneity, an excess modification of lysine (Lys) residues etc. More recently, a recombinant albumin product purified from yeast has been made available on the market. When glycosylated proteins are expressed in a yeast system, they are highly mannosylated with oligosaccharides [8]. Therefore, if genetically engineered glycosylated recombinant HSA (rHSA) could be expressed by a yeast system, the resulting rHSA would contain high levels of the mannosylated form. These novel glycoproteins would be expected to be useful as a carrier for liver-selective therapeutics *via* MR. However, the production of rHSA that is genetically engineered to contain oligosaccharides and its therapeutic application has not been investigated.

Hepatic ischemia/reperfusion (IR) injury is a major clinical problem during perioperative periods and occurs frequently after major hepatic resection or liver transplantation. A growing body of evidence exists to suggest an impaired production of nitric oxide (NO) is a significant contributor to the pathogenesis of hepatic IR injury. As a result, a new strategy involving the delivery of NO to the liver has received much attention for the prevention of hepatic IR injury. *S*-nitrosylated proteins have several advantages over other NO donors. For example, they represent endogeneous NO reservoirs circulating in the blood [9], they induce minimal oxidative stress and high doses are not required to improve recovery from IR induced organ dysfunction [9]. In fact, we (and others) recently found that the administration of *S*-nitrosylated HSA (SNO-HSA) and derivatives thereof to animals with hepatic IR injury significantly reduce the extent of tissue damage [10], although the same concentrations of low molecular weight *S*-nitrosothiols produced no obvious protective effect on hepatic IR injury [11]. Therefore, it would appear that the targeted delivery of SNO-HSA to liver non-parenchymal cells would be a more effective approach to inhibiting liver injuries that are induced by IR.

The objective of this study was to develop novel, genetically engineered Man-rHSA mutants that have the potential to deliver therapeutics to the liver *via* MR localized on liver non-parenchymal cells. These molecules were prepared by inserting the consensus sequence for the *N*-glycoside binding motif using the above three genetically glycosylated variants as a template and a *Pichia pastoris* expression system, which resulted in the production of highly mannosylated forms of the protein. In this study, single mutants (D63N, A320T or D494N) and their triple mutant (TM: D63N/A320T/D494N) rHSAs were produced as candidates for use as liver-selective carriers and their physicochemical and pharmacokinetic properties were examined. Then, to address the potential of the molecules as carriers for liver-selective therapeutics, TM-rHSA-NO conjugate, *S*-nitrosylated TM-rHSA was prepared and its cytoprotective effect was examined using hepatic IR injury model rats.

2. Materials and methods

2.1. Materials and animal

Blue Sepharose 6 Fast Flow was obtained from GE Healthcare (Tokyo, Japan). Enzymes for DNA assays were obtained from Takara (Kyoto, Japan). The *Pichia* Expression kit was obtained from Invitrogen (Carlsbad, CA). Diethylenetriamine-pentaacetic acid (DTPA) was obtained from Dojindo Laboratories (Kumamoto, Japan). $^{111}InCl_3$ (74 MBq/ml in 0.02 N HCl) was a gift from Nihon Medi-Physics Co., Ltd. (Tokyo, Japan). Collagenase (type4) was obtained from Sigma Chemicals Inc. (St. Louis, MO, USA). All other chemicals were of the highest commercial grades available. Sprague–Dawley (SD) rats (180–210 g) were purchased from Kyudou Co. (Kumamoto, Japan). ddY mice were purchased from Japan SLC inc. (Saga, Japan). SD rats and ddY mice were maintained in a temperature-controlled room with a 12-hour dark/light cycle and free access to food and water. All animal experiments were performed according to the guidelines, principles, and procedures for the care and use of laboratory animals of Kumamoto University.

2.2. Generation of *P. pastoris* producing recombinant HSAs

The expression vector pPIC9-wild-type rHSA containing the wild-type rHSA expression cassette stably integrated into chromosomal DNA was used to produce rHSA [12]. The mutants were produced using a QuikChange XL site-directed mutagenesis kit (Stratagene, La Jolla, CA), with the following mutagenic primers (sense and antisense): 5′-GCTGAAAATTGTAACAAATCACTTCATACC-3′ and 3′-GGTATGAAGTGATTTGTTACAATTTTCAGC-5′ (D63N), 5′-GCAAAAAC-TATACTGAGGCAAAGG-3′ and 3′-CCTTTGCCTCAGTATAGTTTTTGC-5′ (A320T), 5′-GCTCTGGAAGTCAATGAAACATACG-3′ and 3′-CGTATGTTTCATTGACTTCCAGAGC-5′ (D494N). D63N/A320T/D494N was made by mutation of all mutation points. *P. pastoris* GS115 his4 was transformed with SalI-digested pPIC9-wild-type rHSA or pPIC9-mutant rHSAs by electroporation according to the manual (EasySelect *Pichia* Expression Kit Version A; Invitrogen). Histidine-independent transformants were selected and subsequently screened for slow methanol utilization phenotypes. Positive clones were induced by treatment with methanol and screened for the production of wild-type or mutant rHSAs by 10% SDS-PAGE of the culture medium.

2.3. Production and purification of recombinant HSAs

The protocol used to express the rHSA was a modification of a previously published protocol [12]. Single colonies of *P. pastoris* were grown (30 °C, 210 rpm, 48 h) in 300 ml of BMGY growth medium (1% yeast extract, 2% peptone, 100 mM potassium phosphate, pH 6.0, 1.34% yeast nitrogen base, 4×10^{-5}% biotin, and 1% glycerol) in 1-liter baffled flasks until an A_{600} value of 2 to 6 was obtained. Cells were then harvested by centrifugation at $3000\times g$, and the cell pellets were washed extensively and resuspended in 300 ml of BMMY medium (1% yeast extract, 2% peptone, 100 mM potassium phosphate, pH 6.0, 1.34% yeast nitrogen base, 4×10^{-5}% biotin, and 1% methanol) to an approximate A_{600} value of 15 to 20. For further culture of this *P. pastoris* suspension, the baffled flasks were shaken (30 °C, 190 rpm, 96 h) with the daily addition (every 12 h) of methanol at a final concentration of 1% to maintain the induction conditions of the alcohol oxidase 1 promoter. The recombinant proteins were purified after 96 h of induction, according to the literature [12]. The protein preparation was first subjected to chromatography with the Blue Sepharose 6 Fast Flow equilibrated with 50 mM sodium phosphate buffer (pH 7.0) after dialysis against the same buffer.

Proteins were further purified using a Phenyl HP column that had been equilibrated with 50 mM sodium phosphate buffer, pH 7.0, containing 0.65 M ammonium sulfate. The column was washed with phosphate buffer (50 mM, pH 7.0) and then eluted with 25 ml of ammonium sulfate in the same buffer (0.65 M). The eluted rHSAs were deionized and defatted by charcoal treatment, freeze-dried, and then stored at −20 °C until used. Sample purity was estimated by a density analysis of Coomassie brilliant blue (CBB)-stained protein bands on 10% SDS-PAGE. The recombinant protein samples of HSA and mutants were estimated to be more than 97% pure.

2.4. Synthesis of mannosylated HSA

Man-(12)-HSA was synthesized by reacting HSA with 2-imino-2-methoxyethyl 1-thioglycomannoside as previously described [13]. The product was dialyzed (molecular weight cutoff, 1000) against ultrapure water, and lyophilized. The number of sugar moieties was controlled by the amount of the sugar derivatives added to the reaction mixture and determined by the anthron method [14].

2.5. Synthesis of glycosylated bovine serum albumin (BSA)

Man-(42)-BSA and Gal-(55)-BSA were synthesized by reacting BSA with 2-imino-2-methoxyethyl 1-thioglycomannoside or thiogalactoside as previously described [13]. Each derivative was purified and concentrated by ultrafiltration (molecular weight cutoff, 10,000) against distilled water, and lyophilized. The number of sugar moieties was controlled by the amount of the sugar derivatives added to the reaction mixture and determined by the anthron method [14].

2.6. CBB-stain and periodic acid Schiff (PAS)-stain of SDS-PAGE

SDS-PAGE was performed using 10% polyacrylamide gel. The gel was stained with Coomassie brilliant blue R250 and Schiff's reagent solution for PAS.

2.7. Circular dichroism (CD) spectra measurement

CD spectra were obtained using JASCO J-720 spectroporalimeter (JASCO, Tokyo, Japan) at 25 °C. Far-UV and near-UV intrinsic spectra were recorded in the range from 200 to 250 nm and from 250 to 350 nm respectively. The protein concentration was determined to be 5 μM (far-UV) or 15 μM (near-UV) in PBS, respectively.

2.8. Pharmacokinetic analysis of recombinant HSAs and chemically modified Man-(12)-HSA

All proteins were radiolabeled with ^{111}In using the bifunctional chelating reagent DTPA anhydride according to the method of Hnatowich et al. [15]. Mice received tail vein injections of ^{111}In-labeled rHSAs and ^{111}In-labeled chemically modified Man-(12)-HSA in saline, at a dose of 0.1 mg/kg. In the early period after injection, the efflux of ^{111}In radioactivity from organs is assumed to be negligible, because the degradation products of ^{111}In-labeled ligands using DTPA anhydride cannot easily pass through biological membranes. This assumption was confirmed by the finding that no ^{111}In was detectable in the urine throughout the 120 min period. At appropriate intervals after the injection, blood was collected from the vena cava under ether anesthesia and plasma was obtained by centrifugation (3000×*g*, 10 min). The liver, kidney, spleen and lung were excised, rinsed with saline and weighed. The radioactivity of each sample was measured in a well-type NaI scintillation counter (ARC-500, Aloka, Tokyo). In the inhibition experiment using mannan, chemically modified Man-(42)-BSA or Gal-(55)-BSA, 50 times volume of mannan (5 mg/kg), 100 times excess of Man-(42)-BSA or Gal-(55)-BSA was simultaneously injected with ^{111}In-rHSAs. The radioactivity of all samples was related (percentages) to the total dose given to the animals.

2.9. Isolation of hepatic Kupffer cells and endothelial cells

The portal vein of rats were cannulated with a polyethylene catheter (diameter, 0.9 mm), and the liver perfused with 125 mL of Hank's balanced salt solution (HBSS) buffer (pH 7.5) without Ca^{2+} at a flow rate of 8 ml/min, then with 100 mL of HBSS buffer (pH 7.5) containing 0.05% collagenase and 4 mM $CaCl_2$ at 37 °C. The liver was minced and suspended in ice-cold HBSS containing 1% (w/v) BSA. The cell suspension was centrifuged 3 times at 50×*g* for 2 min. The supernatant was then centrifuged at 450×*g* for 10 min. The pellets were resuspended in 5 mL of DMEM and layered on top of a two-step Percoll gradient. The gradient consisted of 25% (v/v) Percoll (top) and 50% (v/v) Percoll (bottom). The gradient was centrifuged at 800×*g* for 30 min. Pure non-parenchymal cells banded at the interface between the two density cushions. Pure cultures of Kupffer cells were obtained by seeding purified non-parenchymal cells onto the surface of tissue culture plastic, followed by incubation for 20 min at 37 °C. Pure cultures of endothelial cells were obtained by transferring the nonadherent cells from these dishes to dishes coated with fibronectin, followed by incubation for 1 h at 37 °C. The purity of the isolated endothelial cells or Kupffer cells was assessed by phagocytosis (3 mm latex beads (obtained from Sigma-Aldrich Co. (St. Louis, MO)) or immunostaining (Anti-von Willebrand's Factor antibody produced in rabbit (obtained from Sigma-Aldrich Co. (St. Louis, MO)). The purity of both the isolated endothelial cells and Kupffer cells was over 98%.

2.10. Uptake of HSAs by Kupffer cells and endothelial cells

Endothelial cells isolated from a rat liver, as described above, were plated onto human fibronectin-coated 24-well plates (Becton Dickinson Lab., Bedford, U.K.) at 2×10^6 cells/well, and were grown in serum-free RPMI 1640 for 40 min at 37 °C. Each well was then washed 3 times with 0.75 ml of PBS to remove nonadherent cells, followed by incubation for 2 h with serum-free RPMI 1640. Kupffer cells were plated onto 24-well plates at 1×10^6 cells/well, and grown in Dulbecco's minimal essential medium (DMEM) for 20 min at 37 °C. Each well was then washed 3 times with 0.75 ml of PBS to remove nonadherent cells, followed by incubation for 24 h with DMEM. All cellular experiments were performed at 37 °C in a humidified atmosphere of 5% CO_2 in air. In the uptake experiments, the cells were washed twice with PBS and incubated at 37 °C with 0.5 ml of DMEM supplemented with 3% (w/v) BSA containing the indicated concentrations of ^{125}I-labeled rHSA with or without a 50-fold excess of unlabeled rHSA. The protein was radiolabeled with ^{125}I using the Iodo-gen (1,3,4,6-tetrachoro-3a,6a-diphenylglycoluri) method as previously described [16]. After incubation for 5 h, the culture medium was removed, and the remaining cells in each well were washed three times with 0.75 ml of PBS containing 1% (w/v) BSA, and twice more with PBS. The cells were lysed at 37 °C for 30 min with 0.5 ml of 0.1 M NaOH. One portion of the sample was used to measure the radioactivity of the cell-associated ligand, and the other portion was used to assay cellular proteins using a bicinchoninic acid protein assay (BCA) reagent (Pierce, Rockford, IL).

2.11. S-Nitrosylation of HSA

S-Nitrosylated protein was prepared under conditions that were protected from light and according to previously reported methods [10]. These samples were stored at −80 °C until used. The protein content of all protein preparations used in this study was determined by means of the Bradford assay.

2.12. Cytoprotective effect of SNO-HSAs and chemically modified Man-HSA in vivo

A rat IR liver injury model was employed to investigate the cytoprotective effect of SNO-HSAs and chemically modified Man-(12)-HSA, as previously reported [10]. Saline, as the vehicle control, or SNO-wild-type rHSA or SNO-TM-rHSA or SNO-Man-(12)-HSA (SNO-wild-type HSA, SNO-TM-rHSA and SNO-Man-(12)-HSA were injected at a dose of 0.035 μmol (*S*-nitroso content)/rat) was given *via* the portal vein immediately after the initiation of reperfusion. Plasma alanine aminotransferase (ALT) and aspartate aminotransferase (AST) activities levels were determined by using a transaminase C2 test kit from Wako Chemicals (Saitama, Japan), with activities expressed in international units per liter.

2.13. Western blot analysis

The portal vein of rats was cannulated with a polyethylene catheter (diameter, 0.9 mm), and the liver perfused with PBS. The liver was homogenized using BioMasher (Assist, Tokyo, Japan) with instructions. The resulting pellet is referred to as the liver homogenate. After measurement of the protein content using the BCA protein assay reagent (Pierce, Rockford, IL), each sample was mixed in a loading buffer (2% SDS, 333 mM Tris–HCl (pH 6.8), 10% glycerol,